

First-Principles Analysis of the Effects of Alloying Pd with Ag for the Catalytic Hydrogenation of Acetylene–Ethylene Mixtures

Priyam A. Sheth,[†] Matthew Neurock,^{*,†,‡} and C. Michael Smith[§]

Department of Chemical Engineering and Department of Chemistry, University of Virginia, Charlottesville, Virginia 22904-4741, and The Dow Chemical Company, Freeport, Texas 77541-3257

Received: January 11, 2005; In Final Form: April 26, 2005

The effect of alloying Pd with Ag on the hydrogenation of acetylene is examined by analyzing the chemisorption of all potential C₁ (atomic carbon, CH, methylene, and methyl) and C₂ (acetylene, vinyl, ethylene, ethyl, ethane, ethylidene, ethylidyne, and vinylidene) surface intermediates and atomic hydrogen along with the reaction energies for the elementary steps that produce these intermediates over Pd(111), Pd₇₅Ag₂₅/Pd(111), Pd₅₀Ag₅₀/Pd(111), and Ag(111) surfaces by using first-principle density functional theoretical (DFT) calculations. All of the calculations reported herein were performed at 25% surface coverage. The adsorption energies for all of the C₁ and C₂ intermediates decreased upon increasing the composition of Ag in the surface. Both geometric as well as electronic factors are responsible for the decreased adsorption strength. The modes of adsorption as well as the strengths of adsorption over the alloy surfaces in a number of cases were characteristically different than those found over pure Pd (111) and Ag (111). Adsorbates tend to minimize their interaction with the Ag atoms in the alloy surface. An electronic analysis of these surfaces shows that there is, in general, a shift in the occupied d-band states away from the Fermi level when Pd is alloyed with Ag. The s and p states also appear to contribute and may be responsible for small deviations from the Hammer–Nørskov model. The effect of alloying is more pronounced on the calculated reaction energies for different possible surface elementary reactions. Alloying Pd with Ag reduces the exothermicity (increases endothermicity) for bond-breaking reactions. This is consistent with experimental results that show a decrease in the decomposition products in moving from pure Pd to Pd–Ag alloys.^{2–5} In addition, alloying increases the exothermicity of bond-forming reactions. Alloying therefore not only helps to suppress the unfavorable decomposition (bond-breaking) reaction rates but also helps to enhance the favorable hydrogenation (bond-forming) reaction rates.

I. Introduction

Ethylene polymerization processes used in the production of polyethylene require that the acetylene impurity content of the ethylene feedstock be less than 5 ppm by volume to help prevent catalyst deactivation.^{6–8} Refined ethylene feedstocks, however, can contain up to 2 vol % acetylene and therefore must first be selectively hydrogenated to convert acetylene into ethylene. This process is generally carried out in a fixed bed reactor over Pd catalysts supported on Al₂O₃ operating at either “front-end” or “tail-end” feed conditions.^{9,10} Front-end acetylene hydrogenation units are run at much higher partial pressures of hydrogen and are restricted to a narrow range of temperatures between 323 and 363 K.^{7,11} The overall pressure for front-end operation is between 1 and 5 atm so as to minimize the over-hydrogenation of ethylene to ethane that leads to product loss as well as runaway reaction conditions. Ethylene hydrogenation is also fairly exothermic and will therefore increase its own rate as it liberates more heat. This will enhance the subsequent unselective reactions. Tail-end acetylene hydrogenation units, however, typically operate at much lower partial pressures of hydrogen where reactor runaway is no longer an issue. The lower partial pressures of hydrogen, however, lead to enhanced formation of carbonaceous deposits, which are precursors to green oil that

blocks active sites and thus lowers the catalyst activity.¹² These challenges limit pure Pd-based catalysts that, when combined with the forecasted increases in polyethylene demand,^{12–14} necessitate the development of alternative catalytic materials with improved performance.

The most successful alternative has been to alloy Pd with a group 1B metal such as Ag or Au.¹² It is now well established that these alloys demonstrate marked improvement in catalyst stability as well as selectivity for ethylene formation. In addition, the alloys minimize green oil formation, are more stable to the concentration fluctuations in the reactant feedstocks, and have longer lifetimes.⁸ As a result, such Pd alloys have replaced the Pd-only catalysts in the industrial hydrogenation of acetylene. More specifically, Pd–Ag alloys have found wide acceptance as replacements for Pd-only catalysts for acetylene hydrogenation^{15,16}

This has therefore resulted in a wealth of studies reporting on the different effects of co-metal additions to Pd.^{2,4,17,18} These studies complement the extensive work carried out over supported Pd catalysts and provide useful insight into the effects of alloying.¹⁰ The published literature on this subject is quite extensive. We try to summarize below some of the key results and unanswered questions to provide the necessary background for our work.

II. Background

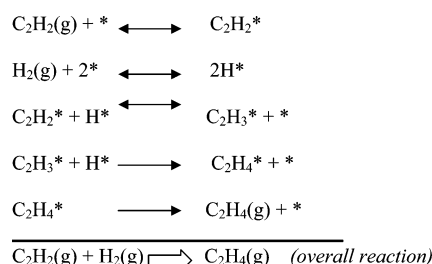
It is generally accepted that acetylene hydrogenation over Pd involves the adsorption of acetylene and hydrogen, sequential

* To whom correspondence should be addressed. E-mail: mn4n@virginia.edu.

[†] Department of Chemical Engineering, University of Virginia.

[‡] Department of Chemistry, University of Virginia.

[§] The Dow Chemical Company.

SCHEME 1

hydrogen addition pathways, and the desorption of ethylene as shown in Scheme 1.^{19,20}

The selectivity of acetylene hydrogenation over ethylene hydrogenation was initially attributed to the overall thermodynamics of adsorption. It was thought that acetylene simply drives ethylene off the surface. This explanation has since been replaced by more detailed mechanistic explanations²¹ to account for the deviations from the classical thermodynamic picture for this process. These explanations can now account for the formation of different surface carbonaceous deposits that arise because of competing secondary reactions. The larger C₈–C₃₀ intermediates that are known as green oil⁴ presumably form because of carbon–carbon coupling and polymerization reactions that can occur on Pd. Different active sites are proposed to catalyze these competing reactions. These deposits are typically nonreactive in that they mainly block the hydrogenation active sites, thus resulting in a loss of catalytic hydrogenation activity. They can also influence the intermolecular competition between acetylene and ethylene.²² Furthermore, the carbonaceous deposit layers are also thought to play a direct role in hydrogenation by allowing other reactions to occur over them.²³ The secondary reaction pathways that are responsible for the initiation of these processes should therefore be included in the analysis of the mechanism. Acetylene hydrogenation is known to be quite sensitive to reaction conditions. The reaction rate models that have been developed are typically applicable only under the narrow range of operating conditions for which they have been constructed, as concluded by Bos and Westerterp.^{9,10} This limited range of operability may be due to the primitive and incomplete description of the elementary steps that comprise the mechanism. Alternatively, this could be due to the breakdown of Langmuir–Hinshelwood models for describing lateral interactions between adsorbates and their influence on the overall kinetics. Under typical operating conditions, the reaction orders for hydrogen and acetylene have been regressed to be 1 to 1.2 and 0.0 to –0.5, respectively. These values are those that are then used in reactor design models.

Similar detailed rate models over Pd-based alloys, however, have yet to be reported in the literature, although kinetic studies over various different Pd alloys^{3,5,17,18,24} are available. Molnár et al.¹² and Coq et al.² have recently reviewed many such studies reporting the effects of different co-metals such as Sn,^{25,26} Cu,²⁷ Pb,²⁸ and Ag^{5,18,24,29} on the hydrogenation of acetylene over Pd. In all of these cases, the second metal is thought to behave predominantly as a spectator wherein the reaction chemistry is still thought to occur at Pd sites. The addition of a second metal reduces the sizes of the Pd ensembles² that form at the surface. This inhibits hydrocarbon decomposition and polymerization reactions, which require larger Pd ensembles. Hydrogenation reactions, however, are structure-insensitive and therefore only weakly affected. The end result is an increase in the selectivity with respect to ethylene upon alloying Pd with Ag. Recent results of the catalytic activity of specific Pd–Ag catalysts for selective acetylene hydrogenation from ethylene feedstocks have

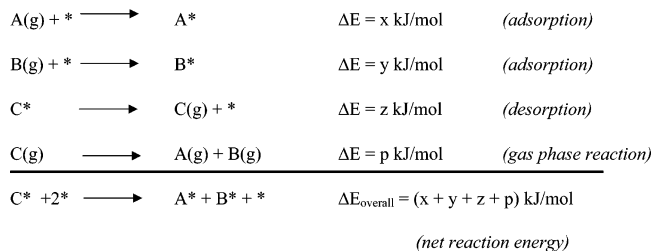
confirmed that alloying them with Ag indeed dilutes the Pd surface ensembles.⁸ Furthermore, the hydrogenation activity and selectivity were found to be higher on catalysts that had higher homogeneous distributions of Ag atoms on the surface. In addition to this ensemble (geometric) effect, alloying can also lead to an electronic effect whereby there is a change in the electronic state of Pd due to its interaction with a second metal. In the case of Pd–Ag, Pd L₃ near-edge experiments (XANES)⁵ show charge transfer from Ag to Pd. Similar charge redistribution results are also reported by Coulthard and Sham³⁰ and by Lu et al.³¹ for Pd–Ag alloys. Charge transfer is thought to weaken the adsorption of the intermediates and thereby alter hydrogenation kinetics and selectivity.

Surface science studies, as well as theoretical studies, have helped further elucidate some of the elementary reaction steps over model surfaces and have begun to provide ideas about the mechanism. This includes adsorption and reaction studies of primary surface intermediates such as atomic hydrogen,^{32–34} acetylene,³⁵ vinyl,³⁶ ethylene,^{37–39} and even secondary intermediates such as ethylidyne⁴⁰ and vinylidene.³⁵ First-principles quantum chemical calculations have been used to examine the modes of adsorption for many of these intermediates on ideal Pd surfaces^{38,41,42} and have begun to provide an understanding of the elementary reaction pathways that occur.⁴² These studies, however, were primarily carried out over pure Pd and do not consider the effects of alloying. Although there are studies on the electronic structure of Pd–Ag alloys³¹ and the adsorption of hydrogen over Pd–Ag,⁴³ a comprehensive analysis of the effect of alloying Pd with Ag on acetylene hydrogenation, to our knowledge, does not exist. An understanding of how the alloy influences the reaction pathways and the mechanism would therefore be important in developing new ideas on improving the selectivity for acetylene hydrogenation.

We report here the results of detailed first-principles DFT calculations of acetylene hydrogenation over Pd and Pd–Ag alloy surfaces. We hope to establish a more quantitative description of the effect of alloying Ag on Pd by calculating the modes of adsorption and the adsorption energies for various surface intermediates as well as the overall reaction energies for relevant elementary steps over model (111) surfaces. These surfaces comprise a range of different Pd/Ag compositions in order to begin to interpret the effect of alloy composition as well as structural arrangements of the metal atoms on the energetics for the hydrogenation of acetylene. This work, however, focuses solely on the overall energetics. Elucidating the kinetics requires the calculation of activation barriers for each of the elementary paths outlined herein.

III. Computational Details

All of the calculations reported herein were performed using gradient-corrected plane wave periodic density functional theoretical methods as implemented in the Vienna ab initio simulation program (VASP).⁴⁴ The interactions between the ions and the electrons were described by Vanderbilt ultrasoft pseudopotentials⁴⁵ using a cutoff energy of 286 eV. Scalar relativistic corrections were incorporated into the pseudopotential used to describe the core electrons. The Kohn–Sham equations were solved self-consistently by using an iterative matrix diagonalization scheme. The electron density was converged using a self-consistent field approach whereby the electronic energy was optimized to within a tolerance of 1×10^{-3} eV. Nonlocal gradient corrections to the total energy were calculated by using the Perdew–Wang 91 exchange correlation potential.⁴⁶ A Monkhorst pack scheme was used to generate the k-point

SCHEME 2

grid. Various k-point meshes were examined for the calculations reported here. A $5 \times 5 \times 1$ grid was found to be accurate as well as computationally efficient. Moving from a $5 \times 5 \times 1$ to a $7 \times 7 \times 1$ grid led to changes in energies that were smaller than 0.01 eV. The time required for convergence, however, was significantly longer for the $7 \times 7 \times 1$ grid. All subsequent calculations were therefore performed using the $5 \times 5 \times 1$ grid.

A detailed accounting of the kinetics for acetylene hydrogenation over supported Pd, Pd–Ag alloys, and Ag will ultimately require tracking the kinetics and dynamics over supported particles. Herein we focus on the intrinsic reaction chemistry over idealized model (111) surfaces in order to provide simple but direct comparisons between the Pd, Pd–Ag alloy, and Ag surfaces. These Pd, Pd–Ag alloy, and Ag surfaces were modeled using 2×2 super cells as (111) surfaces. The (111) surface is

the most close-packed structure for both of the fcc lattices of Pd and Ag. The Pd and Ag metal surfaces were modeled using a three-layer slab. The top two metal layers of the slab along with the adsorbates were allowed to relax in order to model any surface relaxation that may accompany adsorption or surface reaction. The bottom layer was held fixed at the bulk positions of palladium to maintain the structure of the slab. Subsequent calculations using four metal layers showed that the adsorption energy changed by less than 5 kJ/mol. Three metal layers were therefore used to model the surface. A vacuum layer of 12 Å was used to ensure that there were no interactions between the surface adsorbates of one layer and the next slab. The alloy surfaces were constructed by replacing the Pd atoms in the top surface layer with Ag atoms and reoptimizing the unit cell size to establish its new lattice constant. The bottom two layers of the slab, however, are still all Pd. Therefore, there was little change in the optimized lattice parameter because the slab is still primarily Pd.

The overall reaction energy for a particular step is calculated using a Haber cycle approach as outlined in Scheme 2. This method isolates individual reactant or product species and calculates the ideal reaction energy from adsorption energies of the reactants and products along with the gas-phase reaction energy. This scheme isolates coadsorbed reactants (or products), thus removing any interactions between the two coadsorbates.

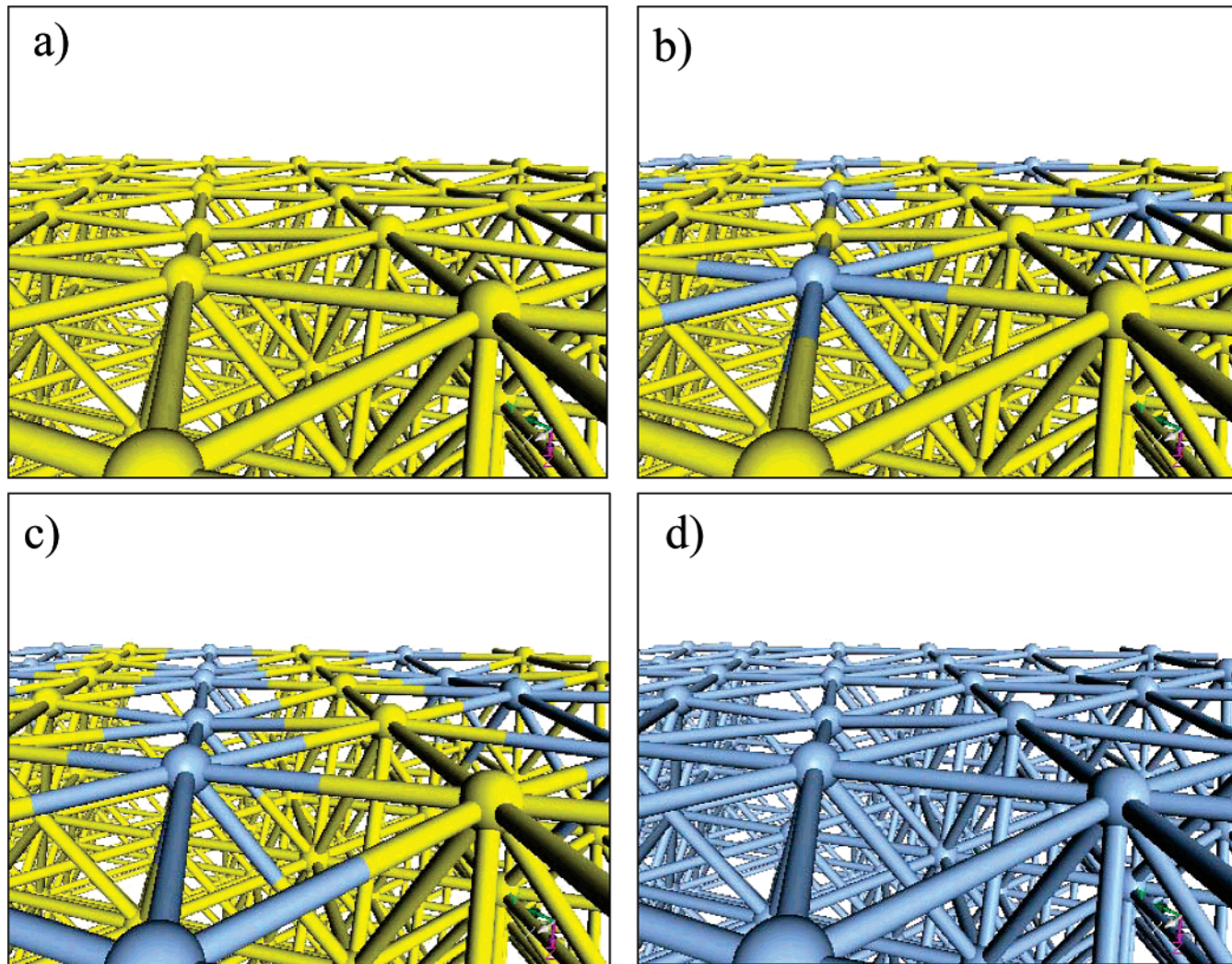
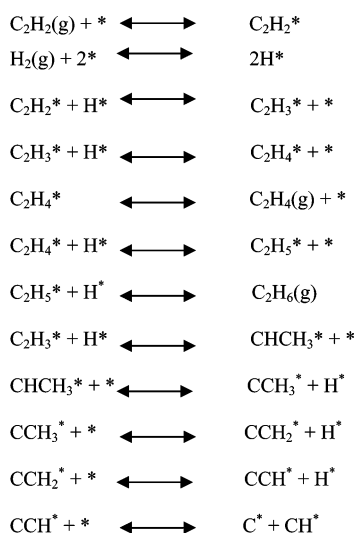


Figure 1. Closed-packed (111) surfaces of (a) Pd, (b) Pd_{75%}Ag_{25%}, (c) Pd_{50%}Ag_{50%}, and (d) Ag used to study the adsorption characteristics of the different intermediates involved in acetylene hydrogenation.

SCHEME 3

Lateral interactions between reactants and other surface adsorbates can have a marked impact on the observed kinetics. These effects are important and would certainly need to be addressed in developing a kinetic model. The aim of this paper, however, is to examine the intrinsic surface energetics. We therefore calculate the reaction energies here by way of the cycle given in Scheme 2.

Per these conventions, a negative value for the reaction energy or adsorption energy indicates that a particular step is exothermic and thus releases heat. The calculated energies here refer only

to the change in the electronic energy at 0 K. Although this provides an estimate of the overall heat of reaction, the actual heat of reaction would require the calculation of zero-point energies along with the energies necessary to go from 0 K to the specified reference temperature.

IV. Results and Discussion

The four surfaces shown in Figure 1 were examined to elucidate the effects of alloying on acetylene hydrogenation: Pd(111), Pd_{75%}Ag_{25%}/Pd(111), Pd_{50%}Ag_{50%}/Pd(111), and Ag(111). The different compositions of Ag used for each of these four surfaces thus provide a systematic variation of the Ag composition in the alloy at the exposed metal surface.

We examine the changes in the mode of adsorption, the adsorption energy, and the overall reaction energy for relevant elementary steps in the hydrogenation of acetylene as we increase the surface composition of Ag. As mentioned earlier, the reaction steps in Scheme 1 represent only acetylene pathways. A more detailed set of elementary steps is required to describe the overall mechanism more adequately. One such speculated mechanism is presented here in Scheme 3.

This mechanism considers not only acetylene and ethylene hydrogenation paths but also additional competing side reactions, which can begin to account for the formation of C₂ deposits including ethylidyne, ethylidene, and vinylidene as well as different C₁ deposits.^{3,12} These reactions will likely be modified over different surfaces.

A first step in understanding how alloying affects hydrogenation chemistry is to understand how it influences the chemi-

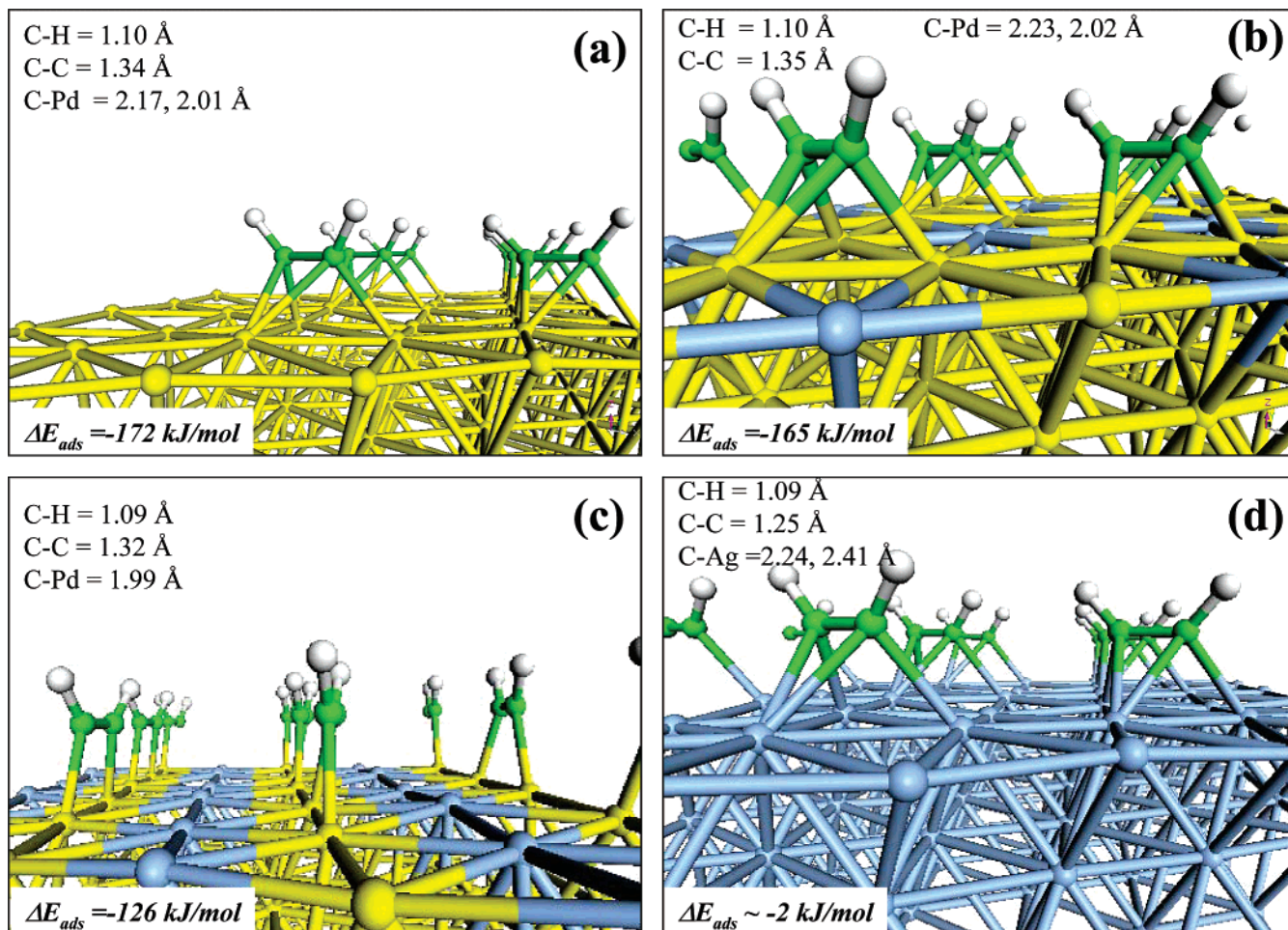


Figure 2. Calculated adsorption geometries of acetylene over (a) Pd(111), (b) Pd_{75%}Ag_{25%}/Pd(111), (c) Pd_{50%}Ag_{50%}/Pd(111), and (d) Ag(111).

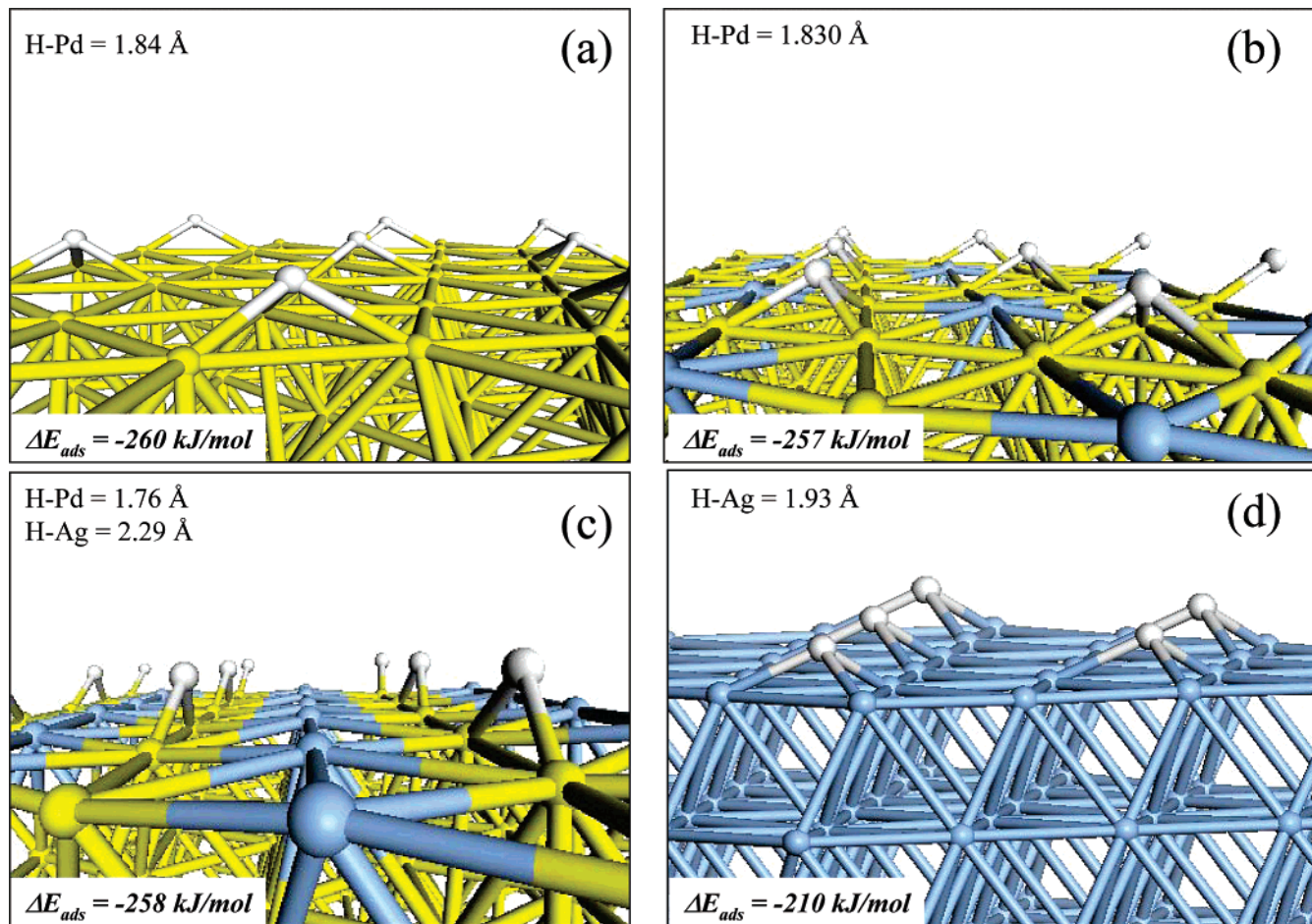


Figure 3. Calculated adsorption geometries of atomic hydrogen over (a) Pd(111), (b) Pd₇₅Ag₂₅/Pd(111), (c) Pd₅₀Ag₅₀/Pd(111), and (d) Ag(111).

sorption of the various surface intermediates that form. The majority of these surface intermediates are C₁ and C₂ species, though C₃–C₃₀ intermediates have also been isolated as reported by Molnar et al.¹² and can lead to deactivation issues. In the present study, however, we focus solely on the C₁ and C₂ intermediates because they can be expected to capture much of what is necessary to describe the influence of alloying on acetylene hydrogenation chemistry. More specifically, we examine the chemisorption of acetylene, vinyl, hydrogen, ethylene, ethyl, ethane, ethylidene, ethylidyne, vinylidene, atomic carbon, CH, methylene, and methyl over the Pd(111), Pd–Ag alloy, and Ag(111) surfaces discussed above. For ease of description, these intermediates are classified here as either primary or secondary. Primary intermediates are defined as those that are involved in the sequential hydrogenation of acetylene to ethylene and ethylene to ethane. These include acetylene, hydrogen vinyl ethylene ethyl, and ethane. Secondary intermediates are all other C₁ and C₂ intermediates that can form at the surface during reaction, including ethylidyne, ethylidene, vinylidene, vinylidyne, C, CH, CH₂, and CH₃.

The adsorption of each of these proposed intermediates was examined at different sites and at different alloy compositions to establish the chemisorption energies as well as overall reaction energetics. The results on the alloys are compared with our earlier results over pure Pd(111).^{36,42}

A. Effects of Alloying on the Chemisorption. 1. Primary Intermediates. (a) HC≡CH (Acetylene). Under UHV conditions, acetylene preferentially adsorbs at the 3-fold hollow sites on Pd(111).^{47,48} We calculate the adsorption energy for acetylene at this site to be −172 kJ/mol for a 2 × 2 adlayer.³⁶ The C–C

bond length for acetylene increases from 1.21 Å in the gas phase to 1.34 Å when it adsorbs at the fcc site as seen in Figure 2a.³⁶ This increase of 0.13 Å in bond length is in agreement with other studies for acetylene on Pd that reported an increase in the C–C bond of 0.14 Å.⁴⁹ The carbon atoms rehybridize from an sp configuration to one that is somewhere between sp² and sp³. The C–C bond takes on more double bond character with a bond length of 1.35 Å that is more characteristic of an sp² configuration. There are four bonds, however, to each carbon atom, which is more characteristic of an sp³ configuration. The C–C bond takes on more double bond character whereby each C atom interacts with two Pd atoms. The C–H bonds in this structure are distorted out of the initial plane of the molecule as the hydrogen atoms tilt away from the metal surface. The C–H bond lengths were calculated to be 1.1 Å.

On the Pd₇₅Ag₂₅/Pd(111) surface alloy, acetylene preferentially adsorbs at the all-Pd 3-fold fcc sites (Pd₃) without any direct interaction with Ag as shown in Figure 2B. The binding energy of acetylene on Pd₇₅Ag₂₅/Pd(111) decreases by 12 kJ/mol from that on the Pd(111) surface (−165 kJ/mol). This minor decrease in the binding energy arises from the electronic effect due to nearest-neighbor Ag atoms. On the Pd₅₀Ag₅₀/Pd(111) alloy shown in Figure 2C, acetylene once again prefers to adsorb only on the Pd atoms. Upon optimization, acetylene shifts from the 3-fold fcc site on the pure Pd(111) surface to the Pd–Pd bridge site on Pd₅₀Ag₅₀/Pd(111). The adsorption energy of acetylene decreases to −126 kJ/mol. This is predominantly due to the change in adsorption site and is thus due to an ensemble effect. The carbon atoms on acetylene are sp² hybridized when bound to the Pd₅₀Ag₅₀/

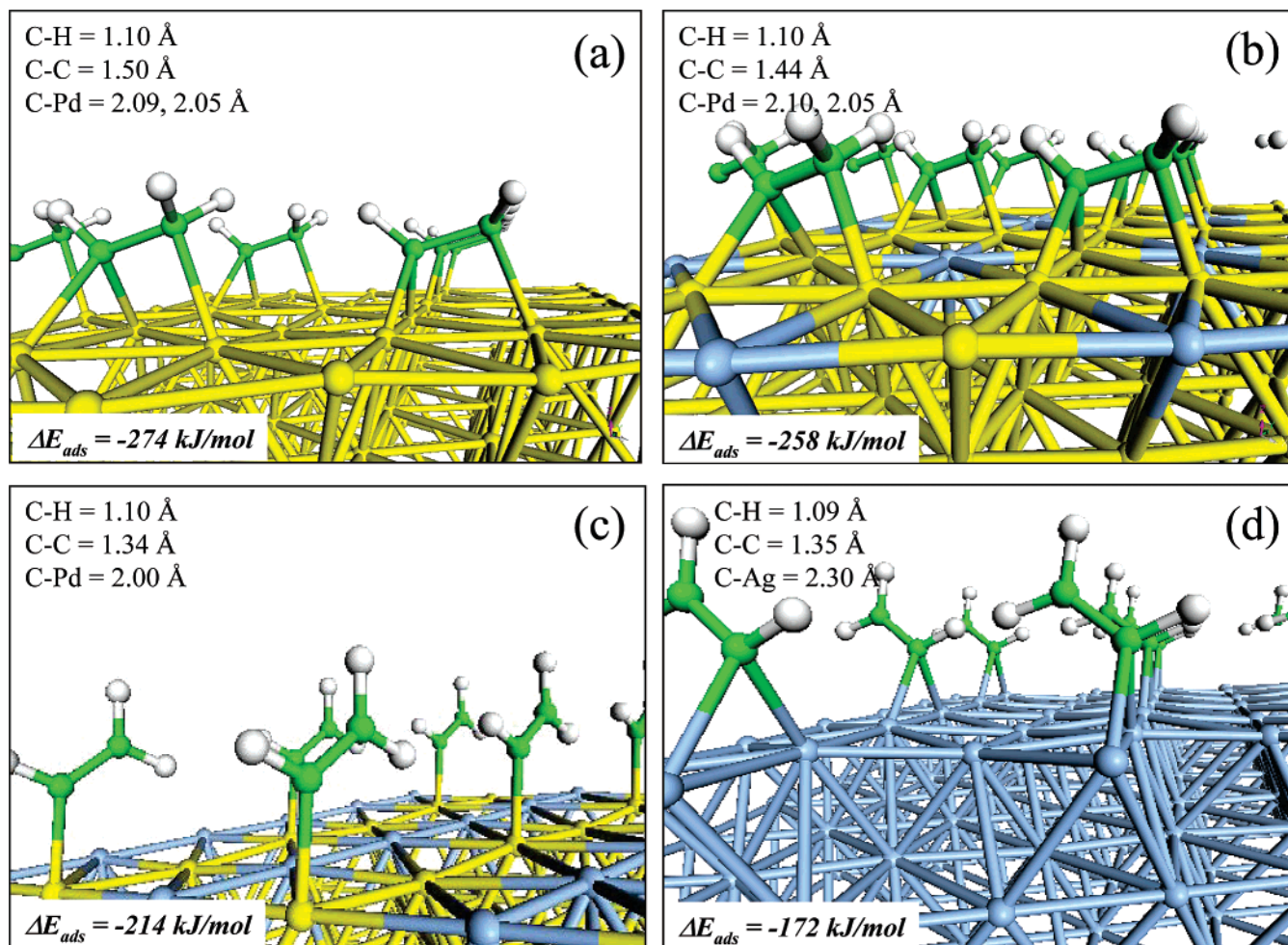


Figure 4. Calculated adsorption geometries of vinyl over (a) Pd(111), (b) Pd_{75%}Ag_{25%}/Pd(111), (c) Pd_{50%}Ag_{50%}/Pd(111), and (d) Ag(111).

Pd(111) surface. On the pure Ag(111), acetylene adsorbs back at the 3-fold fcc site on Ag(111) through a very weak physisorbed interaction. The adsorption energy now decreases to $\sim -2 \text{ kJ/mol}$.

(b) H (Atomic Hydrogen). Molecular hydrogen dissociatively adsorbs over Pd(111) at the 3-fold hollow site.³² This was studied in some detail by Dong and Hafner,³² who suggest that the barrier for H₂ activation is less than 20 meV over the atop, bridge, and 3-fold sites on Pd(111). The dissociative activation of hydrogen over Pd, therefore, can proceed at low temperature. On pure Ag(111), dissociative hydrogen adsorption is an activated process, and the resulting hydrogen atoms formed upon dissociation prefer to sit at the fcc sites as was found on the pure Pd(111) surface.^{33,34} The dissociation of hydrogen over Pd results in the formation of two hydrogen adatoms that prefer to bind at neighboring 3-fold fcc sites (Figure 3). This dissociative adsorption was previously suggested to require only two adjacent vacant sites over Pd. Recent results by Rose et al.,⁵⁰ however, have demonstrated the requirement of at least three vacant hydrogen sites for the adsorption of hydrogen. In any case, the binding energy for atomic hydrogen on Pd was found to be -260 kJ/mol .³⁶ The resulting H–Pd bond lengths were found to be 1.84 Å. Although the binding energy for atomic hydrogen does not change substantially on increasing the composition of Ag in the surface, the binding site does. Atomic hydrogen prefers to sit predominantly at the sites that are fully comprised of Pd. Similar to acetylene, atomic hydrogen moves from the 3-fold Pd fcc sites on Pd(111) to the bridging Pd–Pd sites on the Pd_{50%}Ag_{50%}/Pd(111) surface in order to reduce

interactions with Ag and maintain strong bonds with Pd. The change in the binding energy for atomic hydrogen in moving from the Pd(111) surface to the Pd_{50%}Ag_{50%}/Pd(111) surface, however, is only 5 kJ/mol. On pure Ag(111), dissociative hydrogen adsorption is a much more activated process, and the resulting hydrogen atoms formed upon dissociation prefer to sit at the fcc sites as was found on the pure Pd(111) surface. The binding energy, however, is now reduced to -210 kJ/mol . This is 50 kJ/mol lower than that on Pd(111).

(c) HC=CH₂ (Vinyl). Vinyl binds most favorably in the $\eta_1-\eta_2$ configuration, which places it directly over the 3-fold fcc site over Pd(111). The adsorption energy for vinyl adsorbed in the 2 \times 2 adlayer on Pd(111) was calculated to be -274 kJ/mol .³⁶ The C–C bond length for adsorbed vinyl was calculated to be 1.50 Å (Figure 4a), which indicates that it takes on more single bond character. The CH₂ carbon atom is sp³ hybridized and binds to one Pd atom. The carbon atom in the C–H group, however, binds to two Pd atoms at a Pd bridge site to maintain the same overall sp³ bond character.

On the Pd_{75%}Ag_{25%}/Pd(111) alloy surface, vinyl prefers to sit at the 3-fold hollow fcc sites consisting only of Pd atoms (Figure 4b). The binding energy is reduced by only 16 kJ/mol to -258 kJ/mol from that on the Pd(111) surface. This reduction is due to the electronic interaction of the nearest-neighbor Ag atoms. If vinyl is initially placed above the 3-fold hollow site, which contains a single Ag atom, then the adsorption geometry restructures to minimize the interactions between vinyl and Ag. The binding energy is significantly weaker at -221 kJ/mol . This is the result of an ensemble or geometric effect.

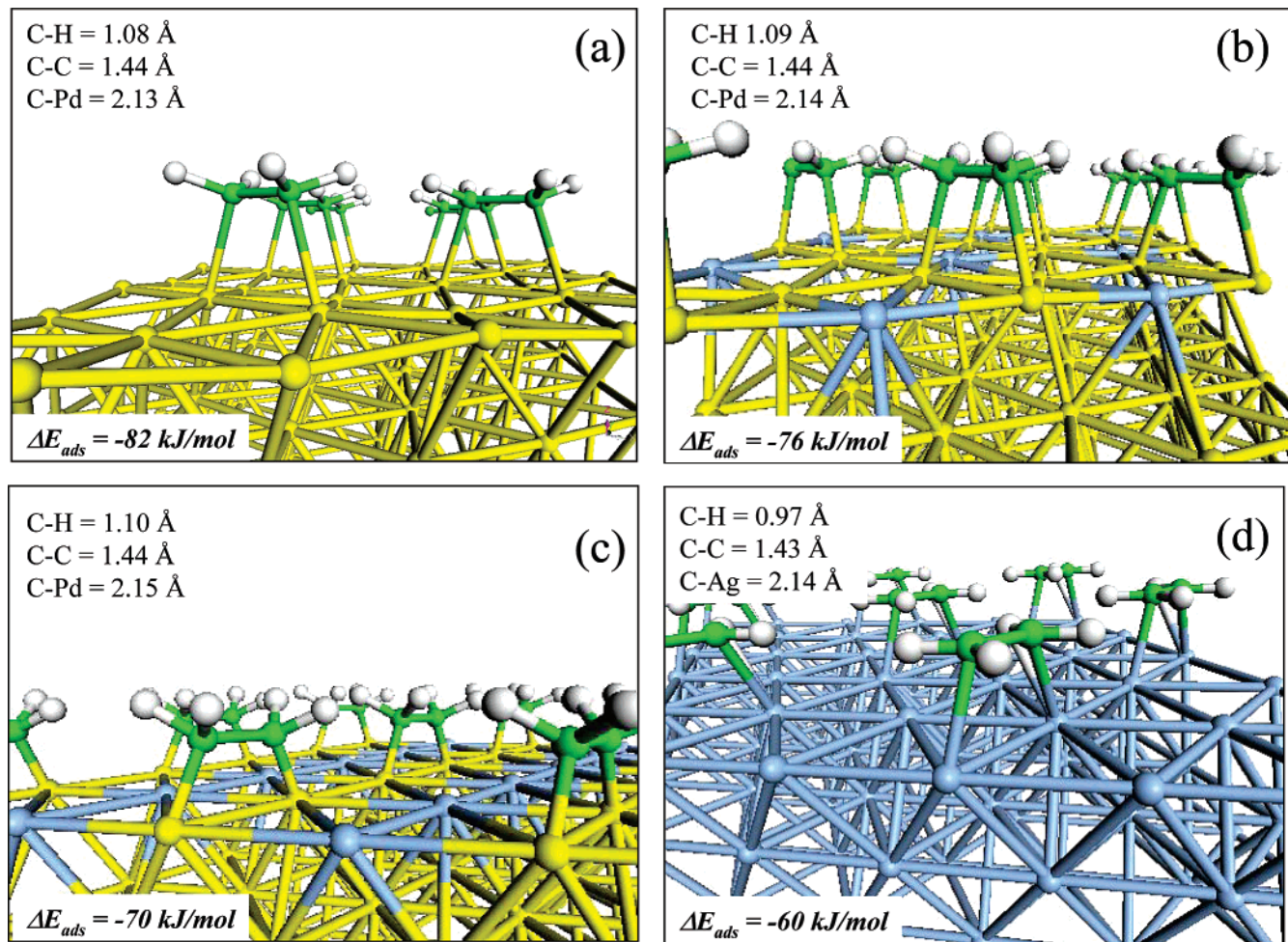


Figure 5. Calculated adsorption geometries of ethylene over (a) Pd(111), (b) Pd₇₅Ag₂₅/Pd(111), (c) Pd₅₀Ag₅₀/Pd(111), and (d) Ag(111).

When the Ag alloy concentration is increased up to 50%, there is a significant change in the structure of the adsorbed surface complex. The CH group shifts from the bridging site on Pd to an atop Pd site (Figure 4c). The carbon atom in the CH group, which is forced to sit atop Pd, can no longer retain an sp^3 configuration on the surface. It therefore converts back to an sp^2 configuration resembling that of ethylene whereby the missing hydrogen atom is replaced by a Pd surface atom. This rotates the vinyl structure by approximately 90° about the C=C bond whereby the Pd atom, the two carbon atoms, and the three hydrogens lie in a plane perpendicular to the surface (Figure 4c). The adsorption energy for vinyl on the Pd₅₀Ag₅₀/Pd(111) alloy is lowered by 60 kJ/mol to -214 kJ/mol. The C-C bond length is now 1.34 Å, and the C-Pd length is 2.0 Å. In moving to Ag(111), the vinyl group is bound at a Ag–Ag bridge site. The vinyl group lies over a 3-fold site in a manner that is somewhat similar to its mode on the Pd(111) surface. There is now, however, a 90° rotation about the C=C bond whereby the terminal CH₂ group is no longer bound to the surface and is oriented perpendicular to the surface (Figure 4d). The carbon atom of the C–H group interacts with a hydrogen atom, the neighboring carbon atom, and two Ag atoms on the Ag(111) surface. The binding energy for vinyl on Ag(111) is decreased to -172 kJ/mol.

(d) H₂C=CH₂ (Ethylene). Under ideal surface conditions, ethylene adsorbs most favorably in the di- σ adsorption mode over Pd(111)^{38,51–53} (Figure 5). The adsorption energy for ethylene in a 2 × 2 overlayer on Pd(111) was calculated to be -82 kJ/mol. Because it interacts only with two Pd atoms, there

is no change in the adsorption configuration of ethylene on the Pd–Ag alloy surfaces studied here (Figure 5b and c) because the two alloy surfaces retain Pd–Pd bridge bonds. The adsorption energy decreases slightly with increasing Ag content. The adsorption of ethylene on the Pd₇₅Ag₂₅/Pd(111) surface was -76 kJ/mol whereas that on the Pd₅₀Ag₅₀/Pd(111) surface was -70 kJ/mol. The slight lowering of the adsorption energy is due to electronic effects. If the coverage of ethylene, however, is increased from 25 to 33%, then the ethylene adsorption energy decreases by 50 kJ/mol, leading to an adsorption energy of -20 kJ/mol on the Pd₅₀Ag₅₀/Pd(111) surface. Ethylene is very weakly held in this configuration. In moving to the Ag(111) surface, ethylene still prefers the di- σ configuration, but the adsorption energy is now reduced to -60 kJ/mol.

(e) H₂C–CH₃ (Ethyl). Ethyl adsorbs in the 2 × 2 ordered overlayer with its CH₂ group bound atop a single Pd atom on the Pd(111) surface, resulting in an adsorption energy of -154 kJ/mol (Figure 6a). Both the surface (CH₂^{*}) carbon atom as well as the CH₃ carbon atom adopt an sp^3 configuration. The C–H, C–C, and C–Pd bond lengths were calculated to be 1.1, 1.45, and 2.19 Å, respectively. It is clear from Figure 6a–d that the adsorbed ethyl does not change its adsorption geometry as the amount of silver in the surface is increased. It does, however, prefer to adsorb atop Pd rather than atop Ag on the two Pd₇₅Ag₂₅/Pd(111) and Pd₅₀Ag₅₀/Pd(111) alloy surfaces. The changes in the adsorption energy are small in moving from Pd(111) (-154 kJ/mol) to Pd₇₅Ag₂₅/Pd(111) (-148 kJ/mol) to Pd₅₀Ag₅₀/Pd(111) (-135 kJ/mol) because the

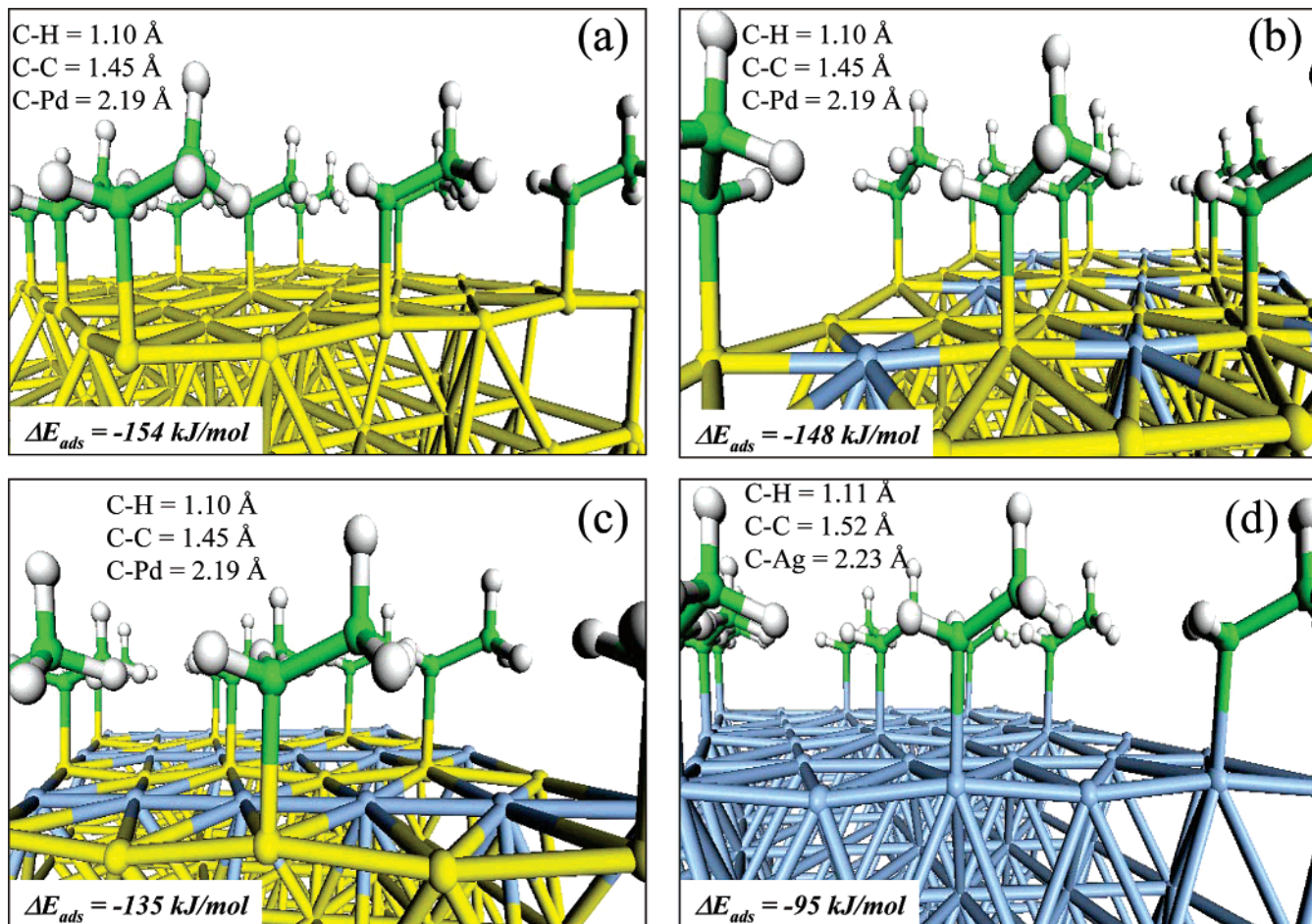


Figure 6. Calculated adsorption geometries of ethyl over (a) Pd(111), (b) Pd₇₅Ag₂₅/Pd(111), (c) Pd₅₀Ag₅₀/Pd(111), and (d) Ag(111).

TABLE 1: DFT-Calculated Site Preferences (SP)^a and Adsorption (Binding) Energies (BE) for the Primary Intermediates over the Different Pd and PdAg Alloy Surfaces

surface adsorbates	Pd(111)		Pd ₇₅ Ag ₂₅ /Pd(111)		Pd ₅₀ Ag ₅₀ /Pd(111)		Ag(111)	
	BE	SP	BE	SP	BE	SP	BE	SP
HC-CH	-172	Pd ₃	-165	Pd ₃	-126	Pd ₂	~ -2	Ag ₃ , Ag ₂ , Ag ₁
HC-CH ₂	-274	Pd ₃	-258	Pd ₃	-214	~ Pd ₁	-172	Ag ₃
H ₂ C-CH ₂	-82	Pd ₂	-76	Pd ₂	-70	Pd ₂	-60	Ag ₂
H ₂ C-CH ₃	-154	Pd ₁	-148	Pd ₁	-135	Pd ₁	-95	Ag ₁
H ₃ C-CH ₃	~ -5	na	~ -5	na	~ -5	na	~ -5	na
H	-260	Pd ₃	-257	Pd ₃	-258	Pd ₂	-210	Ag ₃

^a Pd₃ (Ag₃) – Three-fold fcc site where all three atoms are Pd (Ag). Pd₂ (Ag₂) – Bridge site where both atoms are Pd (Ag). Pd₁ (Ag₁) – Atop site over the Pd (Ag) atom.

adsorption is still through the Pd–C bond. The adsorption energy of ethyl on Ag(111) is lowered to -95 kJ/mol. This is some 59 kJ/mol lower than that for ethyl on Pd(111), and the result is predominantly due to the differences in the Pd–C and Ag–C bond energies.

(f) H₃C-CH₃ (Ethane). Ethane is a fully saturated hydrocarbon and therefore binds to the metal surfaces only through weak van der Waals interactions. The adsorption energies predicted here for ethane over the different Pd alloy surfaces are less than 5 kJ/mol. DFT does not accurately predict van der Waals interactions and therefore underestimates the adsorption of ethane on these metal surfaces. Regardless, the interaction between the fully saturated hydrocarbon and the metal surface is still quite weak.

The adsorption strengths for the primary intermediates on these Pd(111), Pd₇₅Ag₂₅/Pd(111), Pd₅₀Ag₅₀/Pd(111), and Ag(111) surfaces are summarized in Table 1. In general, there

is a consistent decrease in the adsorption energies for all of the primary intermediates with increasing alloy content. This is accompanied by a shift in the adsorption geometries of these intermediates to minimize their interaction with surface Ag atoms. Perhaps the most relevant results for acetylene hydrogenation are the fact that the change in the acetylene adsorption is primarily geometric whereby the substitution of 50% of the surface palladium atoms with silver atoms will, in effect, drive acetylene from the 3-fold fcc hollow site to a Pd–Pd bridge site. This substitution decreases the binding energy of acetylene by 46 kJ/mol. The weaker adsorption energy should help to lower the barrier for hydrogenation, which would increase the rate of acetylene hydrogenation. The influence of Ag on ethylene, however, is predominantly an electronic effect. Even after the substitution of 50% of the surface Pd atoms with Ag atoms, ethylene still prefers the bridge Pd–Pd sites. The change in binding energy in moving from the Pd(111) surface

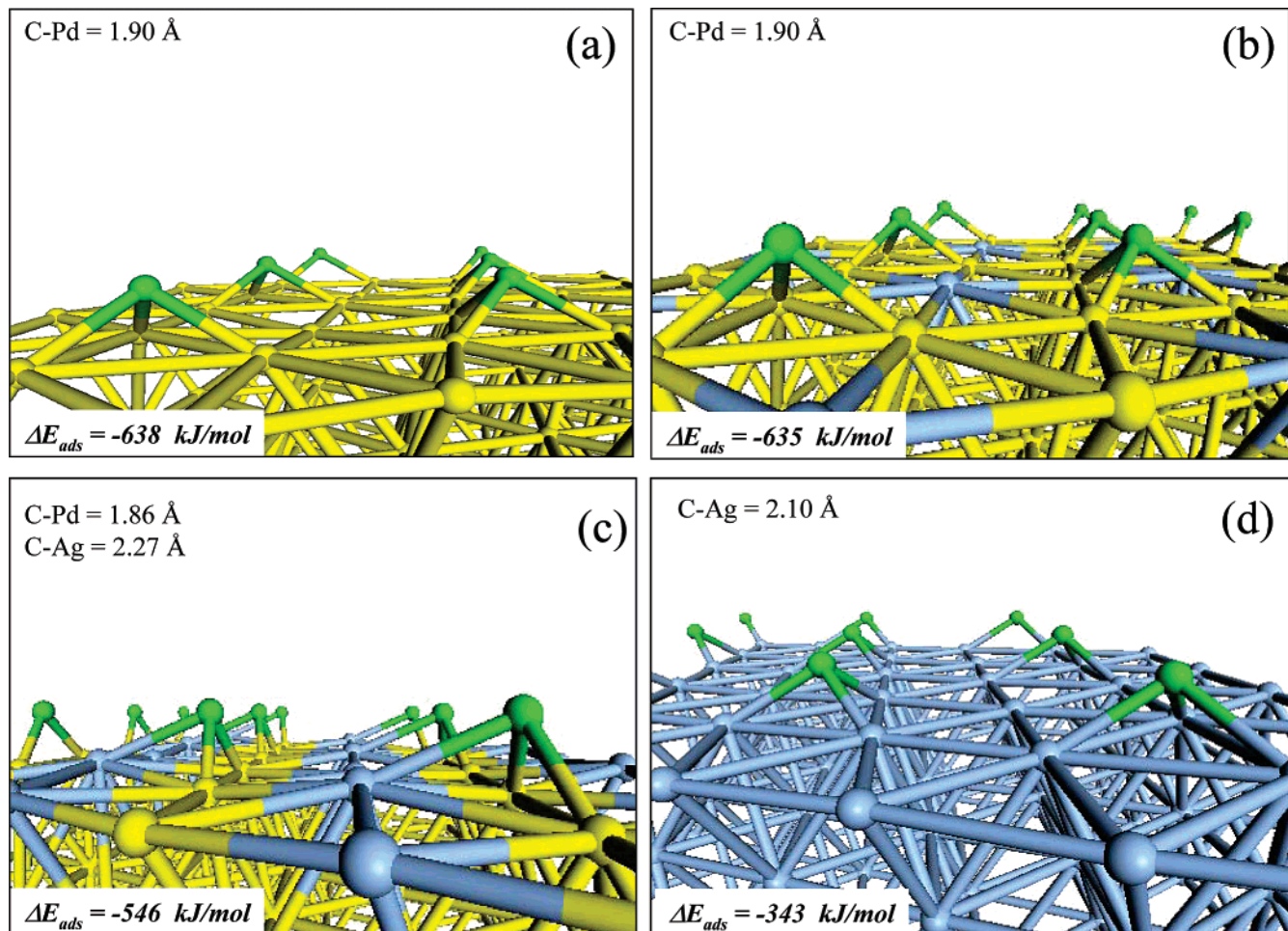


Figure 7. Calculated adsorption geometries of carbon over (a) Pd(111), (b) Pd_{75%}Ag_{25%}/Pd(111), (c) Pd_{50%}Ag_{50%}/Pd(111), and (d) Ag(111).

to Pd_{50%}Ag_{50%}/Pd(111) is only 12 kJ/mol. The influence, therefore, is significantly less and is attributed to electronic interactions. Despite the fact that this is a much smaller decrease in the adsorption energy, it is enough to weaken ethylene enough to begin to drive ethylene off the surface at operating temperatures.

2. Secondary Intermediates. Secondary intermediates, as discussed, are those species that are not directly involved in the Horiuti–Polanyi-like mechanism presented in Scheme 1. These include the C₁ and C₂ intermediates that were not accounted for in Table 1 such as C, CH, CH₂, CH₃, vinylidene, and ethylidene. These intermediates are likely formed via decomposition routes and may readily proceed to form coke or carbonaceous deposits that can block active surface sites and lower catalyst lifetimes. The binding energies for these intermediates over the Pd(111), Pd_{75%}Ag_{25%}/Pd(111), Pd_{50%}Ag_{50%}/Pd(111), and Ag(111) surfaces described above were also examined in detail to understand the effects of alloying.

(a) C (Carbon). Atomic carbon binds strongly to all surfaces examined (Figure 7a–d). As might be expected, it is more strongly bound to Pd than to Ag. The calculated binding energy for carbon in a 2 × 2 overlayer on Pd(111) is −638 kJ/mol, whereas its binding energy on Ag(111) is only −343 kJ/mol. The binding energy of carbon at the all-Pd 3-fold fcc site (Pd₃) on the Pd_{75%}Ag_{25%}/Pd(111) surface is essentially the same as that on the Pd(111) surface. This is due to the fact that there are no direct interactions between C and Ag. Ag is a nearest neighbor where it plays only an electronic role, which appears to be quite small here. The binding energy for C at the 3-fold

fcc sites that contain only one Ag atom (Pd₂Ag) is −546 kJ/mol. Silver plays more of a geometric role in the binding of carbon on the Pd_{50%}Ag_{50%}/Pd(111) surface alloy that contains only bridging Pd sites. The binding energy of carbon decreases by 92 kJ/mol from that on the pure Pd(111) surface. The carbon atom is now in direct contact with silver. This site is therefore much less favorable than the all-Pd 3-fold site. Ag, therefore, reduces the number of available Pd₃ surface sites, which is an ensemble or geometric effect. The adsorption geometry for atomic carbon over all four of the surfaces examined was found to be very similar whereby the carbon atom binds at the center of a 3-fold hollow site. The C–Pd bond length is optimized to be about 1.9 Å.

(b) CH. CH intermediates can form as the result of the activation of the C–C bond of acetylene or via the addition of atomic hydrogen to atomic carbon in the 2 × 2 overlayer. CH prefers the 3-fold fcc sites because this fulfills an sp³ configuration on C (Figure 8a). The binding energy of CH to Pd(111) was calculated to be −632 kJ/mol. The C–Pd bond length is found to be 1.97 Å. CH also prefers the 3-fold hollow sites on both of the alloy surfaces (Figure 8b and c) with similar adsorption structures. There is, however, a small change in the C–Pd and C–Ag bond lengths on the 50% alloy surface. In this case, the C–Pd bond length is reduced to 1.94 Å whereas the C–Ag bond length is increased to 2.21 Å, indicating a stronger interaction of CH with Pd than Ag. The binding energies for CH on these surfaces are lowered by only 5 kJ/mol for the all-Pd 3-fold fcc site on the Pd_{75%}Ag_{25%}/Pd(111) surface (−627 kJ/mol) and by over 77 kJ/mol (−555 kJ/mol) on the

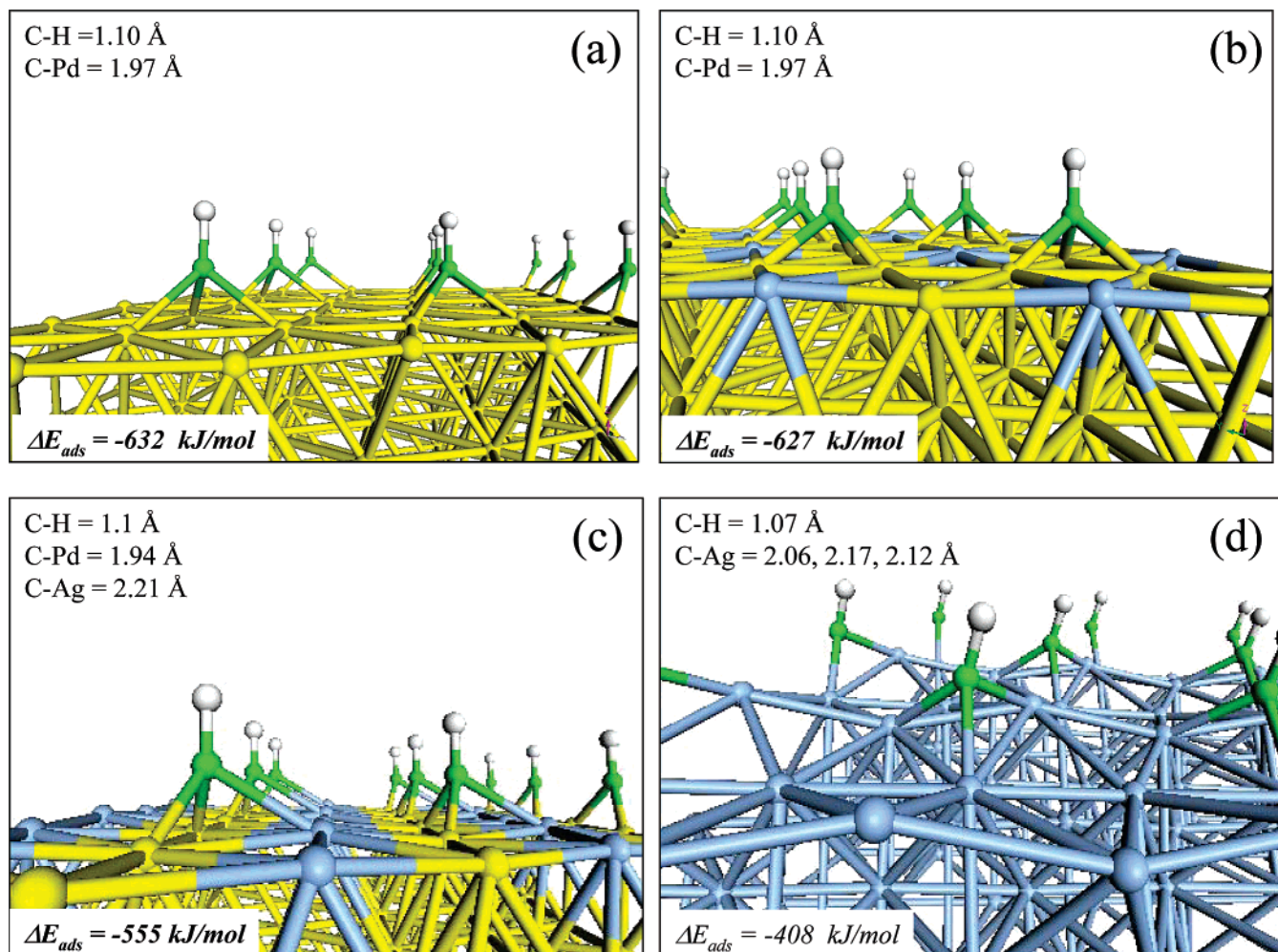


Figure 8. Calculated adsorption geometries of CH over (a) Pd(111), (b) Pd₇₅Ag₂₅/Pd(111), (c) Pd₅₀Ag₅₀/Pd(111), and (d) Ag(111).

Pd₅₀Ag₅₀/Pd(111) surface that contains one Ag atom at each fcc site (Pd₂Ag).

The adsorption of CH on the Ag(111) surface introduces significant distortions in the structure of the surface layer (Figure 8d). This is indicative of the strong restructuring of the Ag surface due to competition between the surface forces and the interactions between CH and the associated Ag atoms. CH preferably binds to the fcc hollow site on Ag(111) with an adsorption energy decrease to -408 kJ/mol .

(c) CH₂. CH₂ intermediates may be the result of either the activation of the C–C bond of ethylene or the hydrogenation of C–H surface intermediates. CH₂ adsorbs in the 2×2 overlayer at the bridge site on Pd(111) (Figure 9a), thus allowing the C atom to take on an sp³ configuration. The optimized C–H and C–Pd bond lengths are 1.10 and 2.02 Å, respectively. The binding energy for CH₂ on Pd(111) is calculated to be -365 kJ/mol . The binding energy for CH₂ adsorbed to the Pd bridge sites on the Pd₇₅Ag₂₅/Pd(111) alloy surface is slightly weaker at -357 kJ/mol . This is the result of a weak electronic effect from the nearest-neighbor Ag atom. The CH₂ binding energy decreases further to -344 kJ/mol in moving to the Pd₅₀Ag₅₀/Pd(111) surface. Although the Pd bridge sites are still the favored adsorption sites, the number of neighboring Ag atoms is increased. The adsorption geometry remains the same over the two alloy surfaces (Figure 9b and c) as well as the Ag(111) surface (Figure 9d). The binding energy for CH₂ on Ag(111) is reduced to -213 kJ/mol , which is 152 kJ/mol lower than that on Pd(111). The large reduction in the binding energy is the

result of the direct interaction between the carbon atom and the Ag surface atoms.

(d) CH₃. CH₃ is quite similar to the ethyl intermediate discussed earlier. CH₃ binds at the atop Pd (or Ag) site on all four of the surfaces studied here for the ideal 2×2 overlayer as can be seen in the results presented in Figure 10a–d. The adsorption energy for CH₃ decreases from -172 kJ/mol over Pd(111) down to -100 kJ/mol over Ag(111). The binding energies over the two alloy surfaces { -168 kJ/mol over Pd₇₅Ag₂₅/Pd(111) (Pd₃ with one nearest Ag atom) and -162 kJ/mol over Pd₅₀Ag₅₀/Pd(111) (Pd₂ with two nearest Ag atoms)} are very similar to that found on the Pd(111) surface. This is not surprising because bonding on each of these surfaces involves the formation of a single Pd–CH₃ bond. Silver is simply just a nearest neighbor and therefore induces only a weak electronic effect.

(e) C–CH₃ (Ethylidyne). Ethylidyne (C–CH₃) is a commonly observed intermediate formed during acetylene hydrogenation, especially under UHV conditions.^{54,55} It is typically unreactive but can decompose to surface carbon at higher temperatures.^{40,54,56} Ethylidyne, adsorbed in the 2×2 structure, preferably binds to the 3-fold fcc hollow site on Pd(111) with a binding energy of -638 kJ/mol (Figure 11a). The C–Pd bond length is 1.99 Å. Ethylidyne adopts a perpendicular orientation on the surface where the C–C bond takes on single bond character. Although the configuration remains the same over the alloy surfaces, there are small shifts in the internal C–C and C–H bond lengths when compared with ethylidyne bound

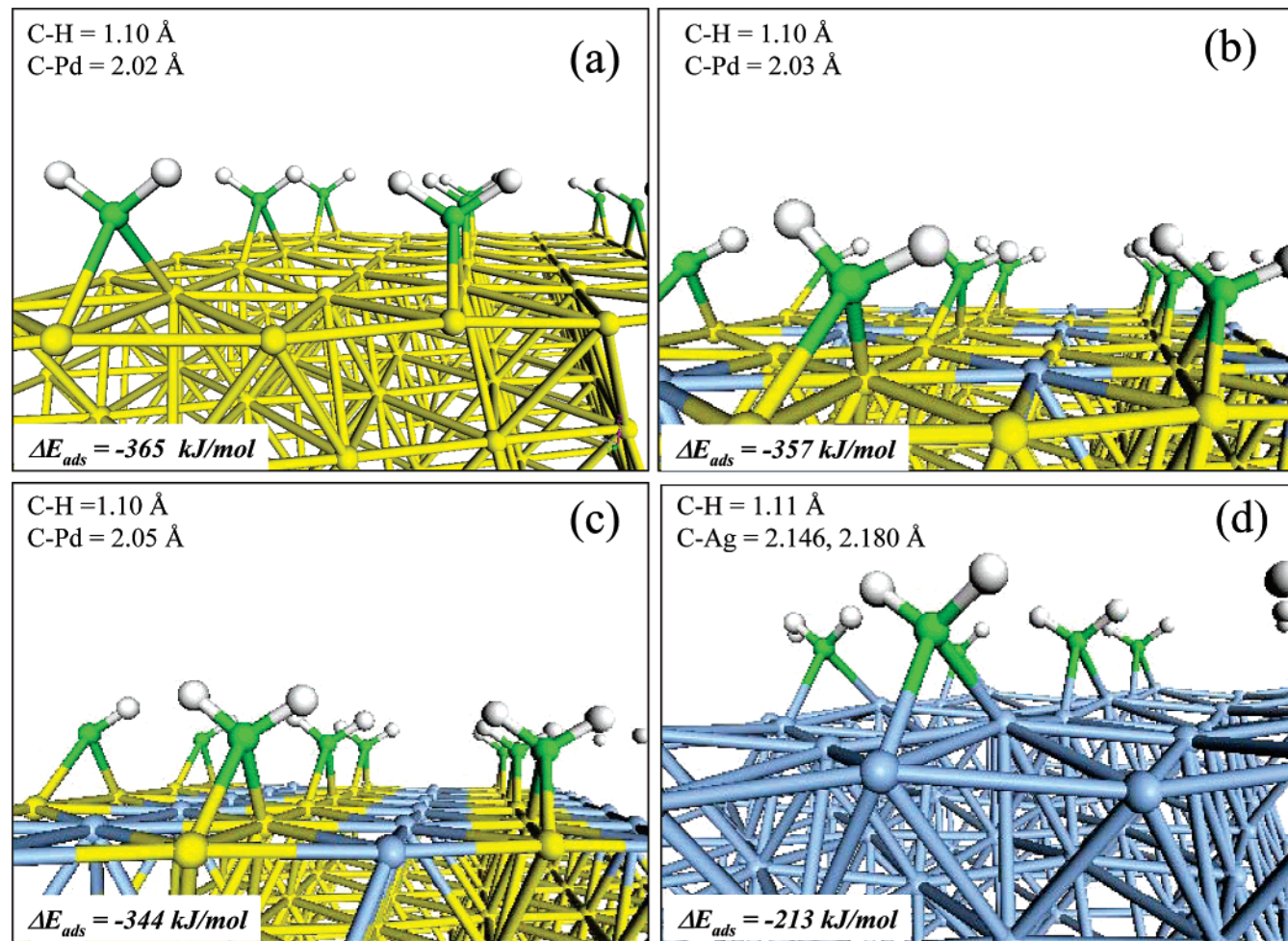


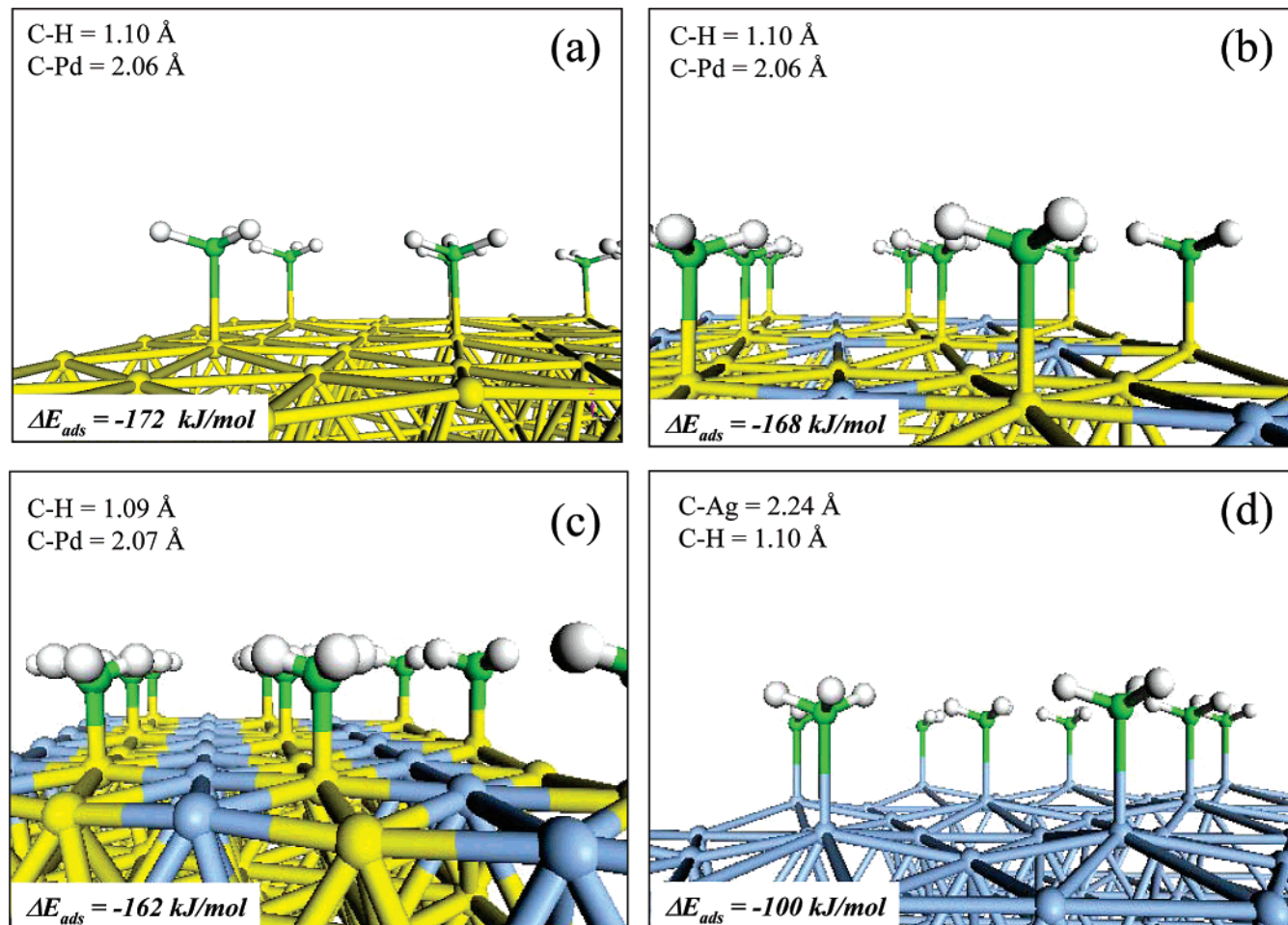
Figure 9. Calculated adsorption geometries of CH_2 over (a) Pd(111), (b) Pd₇₅Ag₂₅/Pd(111), (c) Pd₅₀Ag₅₀/Pd(111), and (d) Ag(111).

to Pd(111) (Figure 11b and c). The binding energy is decreased by only 6 kJ/mol (giving a value of -632 kJ/mol) in moving from the Pd(111) surface to the Pd_{75%}Ag_{25%}/Pd(111). Ethylidene is still preferably bound to three Pd atoms at the 3-fold fcc site. This binding energy decreases by over 119 kJ/mol (giving a binding energy of -557 kJ/mol), however, in moving from the Pd(111) to the Pd_{50%}Ag_{50%}/Pd(111) surface. Ethylidene now binds to the Pd₂Ag site, which is composed of only two Pd atoms and one Ag atom. The binding energy decreases to -402 kJ/mol on the pure Ag(111) surface where ethylidene interacts with three Ag atoms and no Pd atoms. The structure, which is shown in Figure 11d, appears to be quite similar to that for ethylidene on Pd(111).

(f) HC—CH₃ (Ethylidene). Ethylidene (HC—CH₃) has been speculated to be a reactive intermediate in various hydrocarbon reactions over Pd, Pt, and other metals.¹² We examined its binding in detail over different sites on the Pd, Ag, and Pd/Ag alloys. Ethylidene preferentially sits at the bridge site on Pd(111). Ethylidene is simply just a methyl-substituted CH₂ group and therefore binds similarly. The RCH carbon atom binds to the bridge site whereby it can adopt to an sp³ configuration (Figure 12a). The optimized C—C, C—Pd, and C—H bond lengths are 1.50, 2.05, and 1.1 Å, respectively. Ethylidene retains this same configuration on both the Pd₇₅Ag₂₅/Pd(111) and Pd₅₀Ag₅₀/Pd(111) alloy surfaces because these surfaces still have bridging sites composed of two Pd atoms (Figure 12b and c). The binding energy for ethylidene is reduced by only 3 kJ/mol in going from the Pd(111) surface (-330 kJ/mol) to -327 kJ/mol over the

Pd₇₅Ag₂₅/Pd(111) surface. This is due to the fact that Ag is the nearest neighbor and is not directly involved in bonding to ethylidene. The binding energy is reduced by 15 kJ/mol for the Pd₅₀Ag₅₀/Pd(111) alloy surface (-315 kJ/mol). The results for Ag(111) show that the binding energy of ethylidene is reduced to -142 kJ/mol . Ethylidene prefers to sit at the bridge site on Ag as shown in Figure 12d.

(g) C—CH₂ (Vinylidene). Vinylidene (CCH₂) interacts with the Pd surface through both carbon atoms, thus binding to the 3-fold fcc hollow site with a binding energy of -537 kJ/mol . The carbon atom closest to the surface sits at the 3-fold fcc site whereas the CH₂ carbon atom sits directly above a single Pd surface atom resulting in a weaker secondary interaction with the surface. The C—C and the C—Pd bond lengths for the adsorbed vinylidene intermediate were calculated to be 1.29 and 2.04 Å, respectively. The C—Pd distance for the CH₂ carbon atom is measured at 2.39 Å. The binding energy for vinylidene over Pd₇₅Ag₂₅/Pd(111) decreases to -510 kJ/mol . This is likely the result of the weakening or loss of the Pd—CH₂ bond. Vinylidene now stands more perpendicular to the surface with the Pd—CH₂ bond length at 2.97 Å. There is a more marked decrease in the binding energy to -439 kJ/mol , however, in moving to the Pd₅₀Ag₅₀/Pd(111) surface where the 3-fold Pd ensembles are now removed. This change in the binding energy is accompanied by a corresponding change in the adsorption geometry. There is a noticeable shift of the adsorbate away from the Ag atoms. Vinylidene predominantly binds to the bridge site where the Pd—C distance is 2.07 Å. The C—C bond length remains about the same (1.25 Å). The binding energy of

Figure 10. Calculated adsorption geometries of CH_3 over (a) $\text{Pd}(111)$, (b) $\text{Pd}_{75\%}\text{Ag}_{25\%}/\text{Pd}(111)$, (c) $\text{Pd}_{50\%}\text{Ag}_{50\%}/\text{Pd}(111)$, and (d) $\text{Ag}(111)$.**TABLE 2: DFT-Calculated Adsorption Energies (BE) in kJ/mol and Site Preferences (SP)^a of the Secondary Intermediates over the Different Catalytic Surfaces**

surface adsorbates	$\text{Pd}(111)$		$\text{Pd}_{75\%}\text{Ag}_{25\%}/\text{Pd}(111)$		$\text{Pd}_{50\%}\text{Ag}_{50\%}/\text{Pd}(111)$		$\text{Ag}(111)$	
	SP	BE	BE	SP	BE	SP	BE	SP
C	-638	Pd_3	-635	Pd_3	-546	Pd_2Ag	-343	Ag_3
CH	-632	Pd_3	-627	Pd_3	-555	Pd_2Ag	-408	Ag_3
CH_2	-365	Pd_2	-357	Pd_2	-344	Pd_2	-213	Ag_2
CH_3	-172	Pd_1	-168	Pd_1	-162	Pd_1	-100	Ag_1
$\text{C}-\text{CH}$	-405	Pd_3	-408	Pd_3	-329	Pd_2	-296	Ag_3
$\text{C}-\text{CH}_2$	-537	Pd_3	-510	Pd_3	-439	Pd_2Ag	-357	Ag_3
$\text{C}-\text{CH}_3$	-638	Pd_3	-632	Pd_3	-557	Pd_2Ag	-402	Ag_3
$\text{HC}-\text{CH}_3$	-330	Pd_2	-327	Pd_2	-315	Pd_2	-142	Ag_2

^a Pd_3 (Ag_3) – Three-fold fcc site where all three atoms are Pd (Ag). Pd_2 (Ag_2) – Bridge site where both atoms are Pd (Ag). Pd_1 (Ag_1) – Atop site over the Pd (Ag) atom. Pd_xAg_y – Mixed site where x and y denote the number of Pd and Ag atoms, respectively, of the site.

vinylidene on $\text{Ag}(111)$ is lowered further to -357 kJ/mol . It sits at the 3-fold fcc site and is nearly perpendicular to the Ag surface. It prefers the 3-fold hollow sites with the C–Ag distances at 2.34 \AA (Figure 13d).

(h) $\text{C}-\text{CH}$ (Vinylidene). Vinylidene (CCH) formation is speculated to occur by the dehydrogenation of acetylene. Vinylidene in a 2×2 adlayer preferentially binds to the 3-fold fcc sites on $\text{Pd}(111)$ through the bare carbon atom. As can be seen from Figure 14a, there is also a weak interaction with the CH carbon atom, which accounts for its bent geometry. The adsorption energy is calculated to be -405 kJ/mol . The C–C bond distance was measured to be 1.28 \AA . Vinylidene binds to three Pd atoms in the 3-fold fcc site on the $\text{Pd}_{75\%}\text{Ag}_{25\%}/\text{Pd}(111)$ surface. The binding energy remains about the same as that on $\text{Pd}(111)$ at -408 kJ/mol . The optimized C–Pd bond

TABLE 3: Average Reduction in Adsorption Energy for C_1 and C_2 Intermediates Relative to Adsorption Energy on the $\text{Pd}(111)$ Surface^a

Surface Site	$\text{Pd}_{75\%}\text{Ag}_{25\%}/\text{Pd}(111)$	$\text{Pd}_{50\%}\text{Ag}_{50\%}/\text{Pd}(111)$	$\text{Ag}(111)$
Three fold site	7	85	198
Bridge site	6	47	121
Atop site	5	15	66
Geometric and Electronic Effects			
Electronic Effects			

^a The calculated energies are all given in kJ/mol.

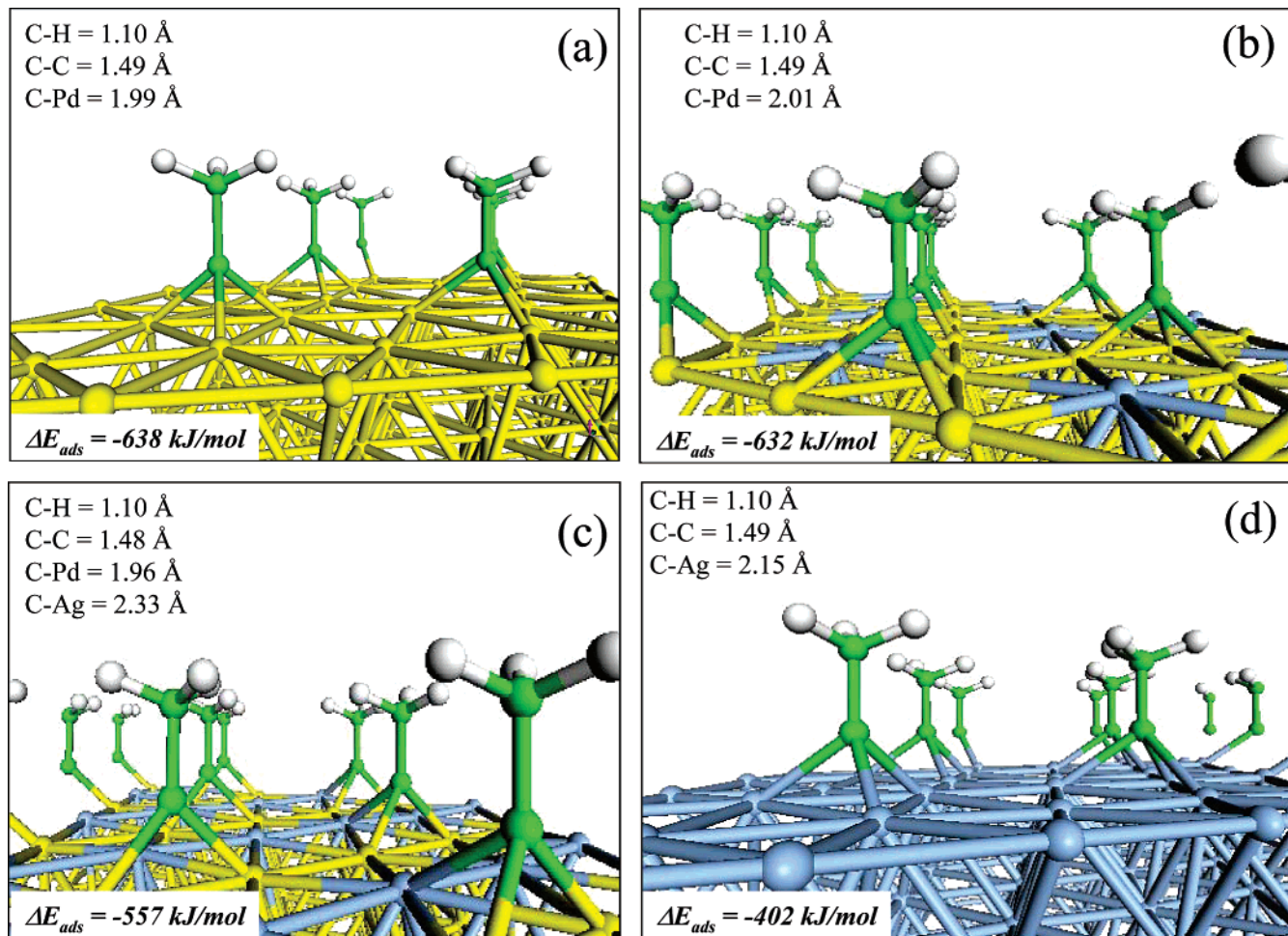


Figure 11. Calculated adsorption geometries of CCH_3 over (a) $\text{Pd}(111)$, (b) $\text{Pd}_{75\%}\text{Ag}_{25\%}/\text{Pd}(111)$, (c) $\text{Pd}_{50\%}\text{Ag}_{50\%}/\text{Pd}(111)$, and (d) $\text{Ag}(111)$.

is 1.25 Å. The adsorption of vinylidyne on the $\text{Pd}_{50\%}\text{Ag}_{50\%}/\text{Pd}(111)$ surface is significantly reduced to -329 kJ/mol . It prefers to interact solely with the Pd atoms and therefore shifts from the mixed Pd_2Ag 3-fold site to the Pd–Pd bridge site (Figure 14c). The binding energy is reduced further to -296 kJ/mol when vinylidyne adsorbs on $\text{Ag}(111)$. It shifts back, however, to the 3-fold fcc site on Ag because there is no longer a preference for specific metal atoms.

B. Electronic and Geometric Ensemble Analysis. The adsorption energies for the primary as well as the secondary intermediates on the different surfaces examined here are summarized in Tables 1 and 2. The results show that there is a consistent decrease in the adsorption energies of these intermediates with increasing surface Ag content. The degree of weakening strongly depends on whether the adsorbates explicitly bond to Ag atoms, change their site preference to avoid interactions with Ag, thus reducing its coordination number with Pd, or simply sit at Pd sites that have Ag neighbors but do not directly contact Ag atoms. This is seen in Tables 1 and 2, which also classify the intermediates studied here according to their binding site over the different surfaces. The intermediates that bind to the 3-fold hollow site show the greatest sensitivity as a result of alloying. This is primarily due to the fact that they interact with the greatest number of surface atoms and require the presence of specific surface ensembles. In some instances, intermediates are forced to bind to lower coordination sites on the alloy surface to minimize their interactions with Ag surface atoms. Expectedly, intermediates that bind to the bridge and atop sites over $\text{Pd}(111)$ are not as strongly affected as a result of alloying, at least at the conditions studied here.

To understand the general trends, we calculated the *average* reduction in the adsorption energy for intermediates bound to the same surface sites over a wide range of alloy compositions. Table 3 tabulates the *average* reduction in the adsorption energy for intermediates bound to the 3-fold, bridge, and atop sites on each of the alloy surfaces. As should be expected, the 3-fold sites show the greatest reduction, followed by the bridge sites and atop sites. The changes in the adsorption energy that result from alloying can be roughly categorized as being the result of either geometric or electronic effects. Geometric effects weaken the binding energy either by direct interactions between the adsorbate and the Ag atoms or through a change in the adsorbate's binding site to remove the interactions with Ag. The results in Table 3 are organized along these lines as well. The changes in the adsorption energies that are ascribed to electronic effects are shown in the lower left-hand side of Table 3, whereas those ascribed predominantly to geometric effects are shown in the upper right-hand side. The results indicate that the geometric effects are significantly greater than the electronic effects in the weakening of the adsorption of different surface intermediates. The binding energy for atomic carbon on Pd, for example, is significantly greater than the binding energy of atomic carbon on Ag. The introduction of Ag into the explicit binding sites therefore markedly decreases the energy of adsorption. In a number of instances, the difference is enough to push an intermediate to lower coordination sites to remove its interactions with Ag and thus increase the strength of the remaining Pd–C bonds.

The change in the electronic properties of the Pd atoms due to nearest-neighbor Ag atoms, however, contributes to only a

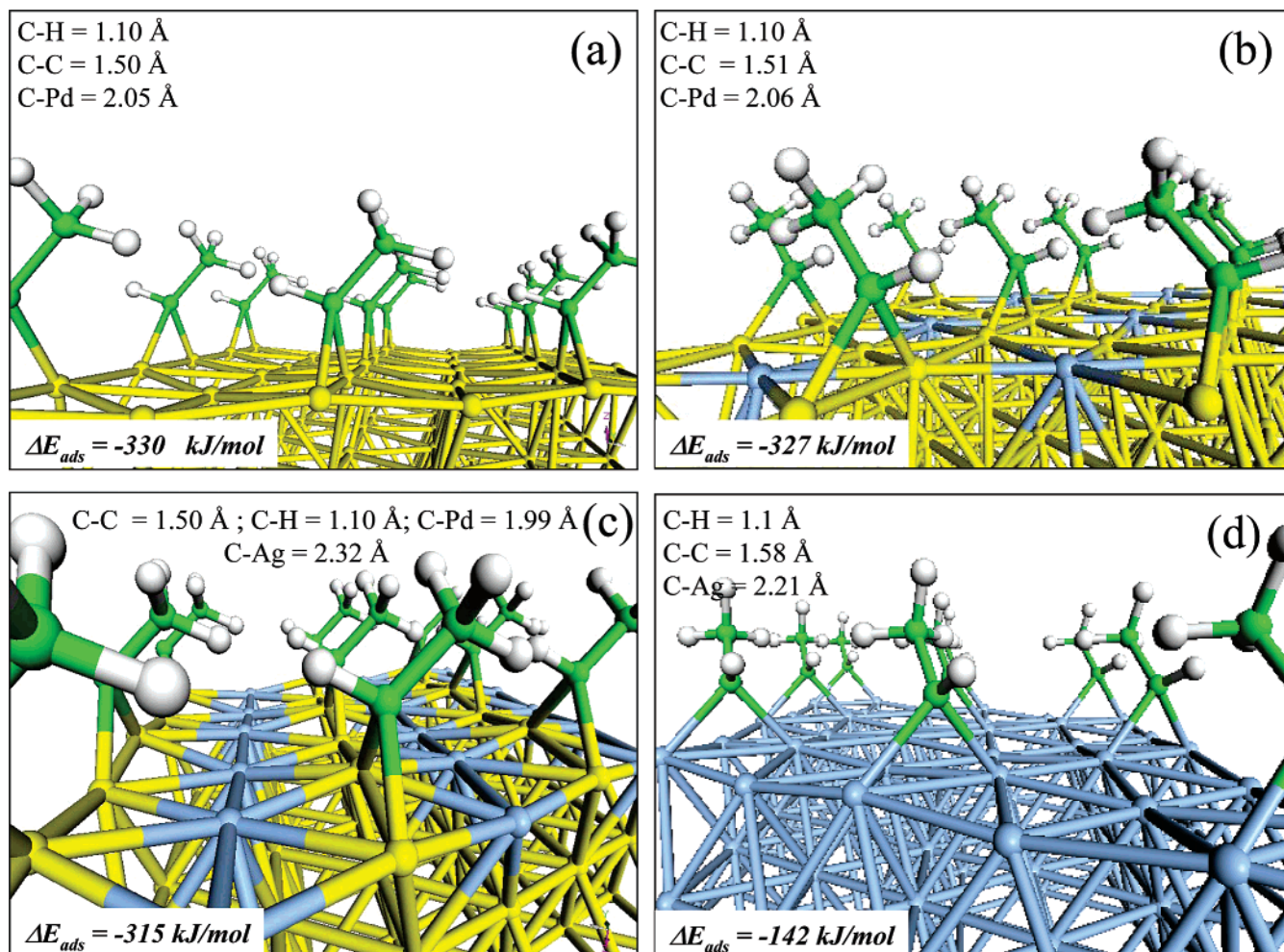


Figure 12. Calculated adsorption geometries of HCCH_3 over (a) $\text{Pd}(111)$, (b) $\text{Pd}_{75\%}\text{Ag}_{25\%}/\text{Pd}(111)$, (c) $\text{Pd}_{50\%}\text{Ag}_{50\%}/\text{Pd}(111)$, and (d) $\text{Ag}(111)$.

small decrease in the adsorption energies. To analyze the electronic effects in more detail, we calculated the local density of states (LDOS) for the d band projected onto the Pd atoms in the surface as we increase the amount of Ag in the surface alloy. This idea was first developed by Hammer and Nørskov¹ to describe the changes in the adsorption energies with changes in the electronic structure for bimetallic pseudomorphic overlayers. We construct local density of states plots for all of the surfaces examined herein to establish the energy states for the s, p, and d states available at the surface atoms. The results for the d states, which are shown in Figure 15, indicate that there is a large density of available d states above the Fermi level in Pd(111) (Figure 15a) and almost no available energy states above the Fermi level for occupation in Ag(111) (Figure 15d). This is expected because Pd is a 4d transition metal whereas Ag is a nearly filled 1B metal. In the case of the two surface alloys, there is a gradual reduction in these available energy states on Pd as the alloy content increases (Figure 15b and c). There is also an accompanying shift in the d-band center¹ away from the Fermi level in moving from Pd(111) to Pd_{75%}Ag_{25%}/Pd(111) to Pd_{50%}Ag_{50%}/Pd(111) to Ag(111). This shift in the d-band center away from the Fermi level is consistent with the d-band center model developed by Hammer and Nørskov.¹ This shift can be used to correlate the reduction in the adsorption energies of different intermediates on the alloy surfaces in an approach used by Pallassana et al.⁵¹ It is important to note that the shift in the d-band center does not monotonically decrease with the surface composition of Ag for the two-alloy surface studied. This may be the result of contributions of s

and p states that contribute to the adsorption. The s and p bands are plotted along with the d states in Figure 15. It is clear that the s and p states are not featureless, as assumed in the strict d-band model, and likely contribute to the bonding. Their relative change, however, is still small compared to those of the d states.

Adsorbates that bond directly to Pd and Ag are influenced by both electronic and geometric effects. The relative magnitude of the geometric effect, however, was found here to be significantly greater than that of the electronic effect. In any case, the *net* effect on the hydrogenation chemistry is a consistent decrease in the adsorption energies of the different surface intermediates with increasing surface alloy content.

C. Reaction Energies. The analysis of the effect of Ag on the hydrogenation of acetylene can be further extended by the evaluation of the reaction energies for the different elementary reactions that can occur over these surfaces. The elementary steps can be broken down into bond-breaking and bond-making processes necessary for acetylene hydrogenation (Table 4). These reactions are composed of the intermediates examined above as either reactants or products. The elementary steps described here are all reversible. Therefore, bond-forming reactions are simply the reverse of bond-breaking reactions and vice versa. We examine the influence of alloying on both bond-forming and bond-breaking reactions.

The reaction energies for each of the different elementary reactions considered herein were calculated using the Haber cycle approach described above. They are tabulated in Table 4 for the four surfaces considered here. The results in section a

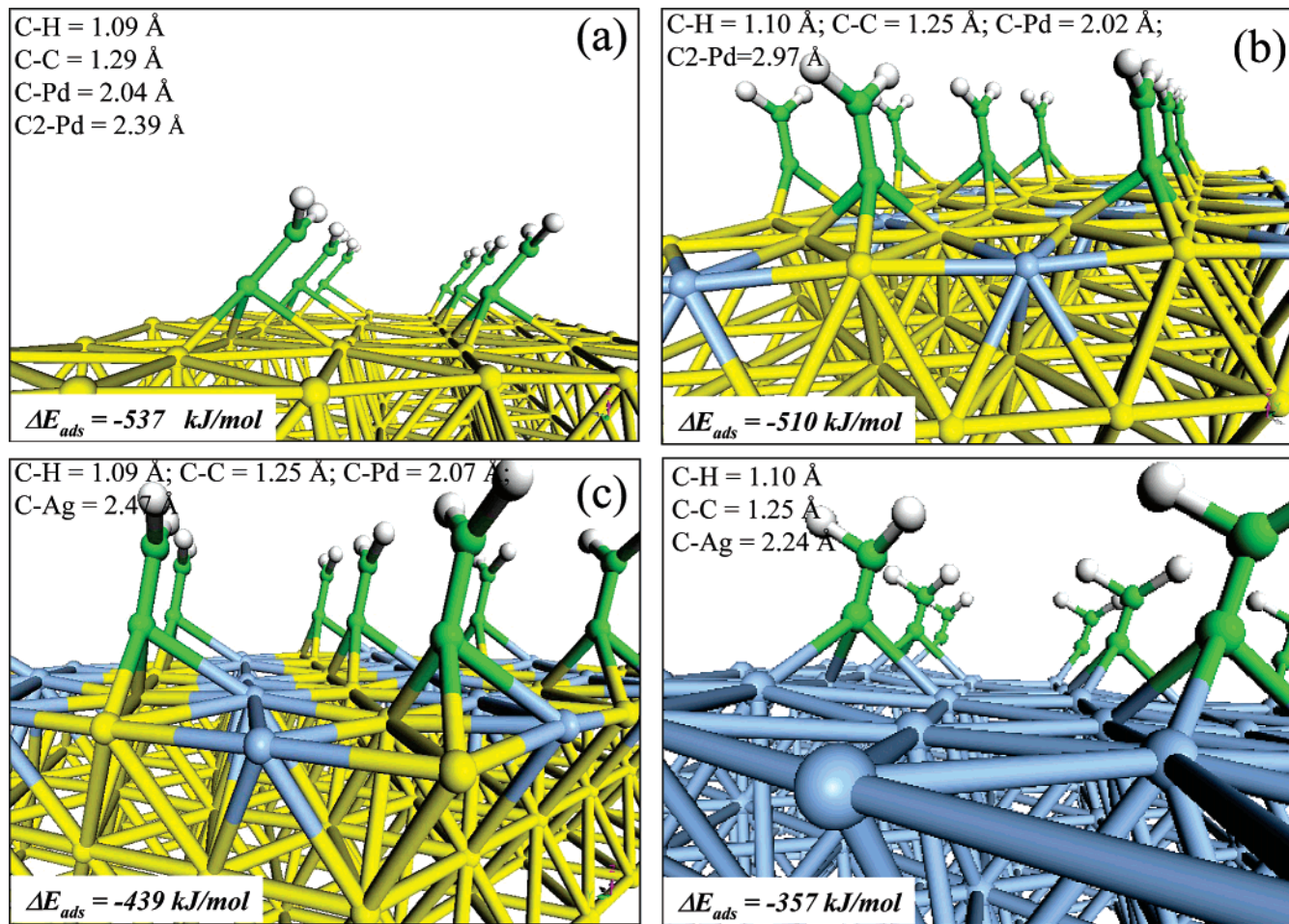


Figure 13. Calculated adsorption geometries of CCH_2 over (a) Pd(111), (b) Pd₇₅Ag₂₅/Pd(111), (c) Pd₅₀Ag₅₀/Pd(111), and (d) Ag(111).

of Table 4 indicate that the bond-breaking reactions, in general, become less favorable with increasing Ag content. For example, vinyl decomposition (bond breaking) to an adsorbed vinylidene and a hydrogen surface intermediate changes from +12 kJ/mol over Pd(111) to +28 kJ/mol over Pd₇₅Ag₂₅/Pd(111) to +52 kJ/mol over Pd₅₀Ag₅₀/Pd(111) to +139 kJ/mol over Ag(111).

The results in Table 4 also show the opposite but analogous trend that bond-forming reactions become more favorable (less endothermic or more exothermic) with increasing Ag content. The hydrogenation of the vinyl intermediate to ethylene, for example, becomes more exothermic with increasing Ag content. The reaction exothermicity increases from -42 kJ/mol over Pd(111) to -55 kJ/mol over Pd₇₅Ag₂₅/Pd(111) to -92 kJ/mol over Pd₅₀Ag₅₀/Pd(111) to -171 kJ/mol over Ag(111).

The general idea that bond-forming reactions become more favorable while bond breaking reactions become less favorable can be used to qualitatively guide our understanding of the influence of alloying on hydrogenation activity and selectivity. On the basis of the principles stated above, the addition of Ag should enhance the hydrogenation (bond-forming) reactions and minimize the unselective bond carbon–carbon bond-breaking steps that lead to the deposition of C_1H_x fragments. This would potentially improve the activity as well as the selectivity. It is important to note, however, that Ag alone does not catalyze acetylene hydrogenation because Ag does not effectively activate hydrogen. Pd is necessary for activating hydrogen.^{32,33} A balance in the Pd/Ag ratio is therefore necessary to help promote specific bond-breaking and bond-making steps to enhance activity and selectivity.

Understanding the selectivity differences between acetylene and ethylene hydrogenation reactions, both of which are bond-forming reactions, is more difficult and would require a detailed analysis of the reaction pathways including the activation barriers over each of the different surfaces. A preliminary analysis considering the overall reaction energetics calculated herein indicates that acetylene hydrogenation to vinyl is nearly thermoneutral over a range of different Pd–Ag compositions except for the pure Ag(111) surface where the reaction is markedly exothermic (-121 kJ/mol). The subsequent reaction of vinyl to ethylene is fairly exothermic even on Pd(111) and increases in exothermicity with increasing Ag content.

The reaction energies for ethylene hydrogenation to ethyl were found to be moderately endothermic over all of the surfaces considered here, thus suggesting that this reaction is less favorable than the initial reaction of acetylene to vinyl. Although the subsequent hydrogenation of the ethyl intermediate to form ethane was found to be exothermic over the full range of PdAg compositions studied, it was also found to be less favorable than the second reaction step in the acetylene hydrogenation sequence of vinyl to ethylene. The addition of Ag, therefore, appears to enhance the reaction of acetylene to vinyl while slightly impeding the subsequent reaction of ethylene to ethyl, at least for the alloys presented here. This should help to increase the selectivity of acetylene hydrogenation to ethylene. These observations require further analysis in that the reaction kinetics now need to be examined. Although these results have been documented over pure Pd(111)^{36,42} surfaces, they remain to be reported over the alloy surfaces. We have recently evaluated

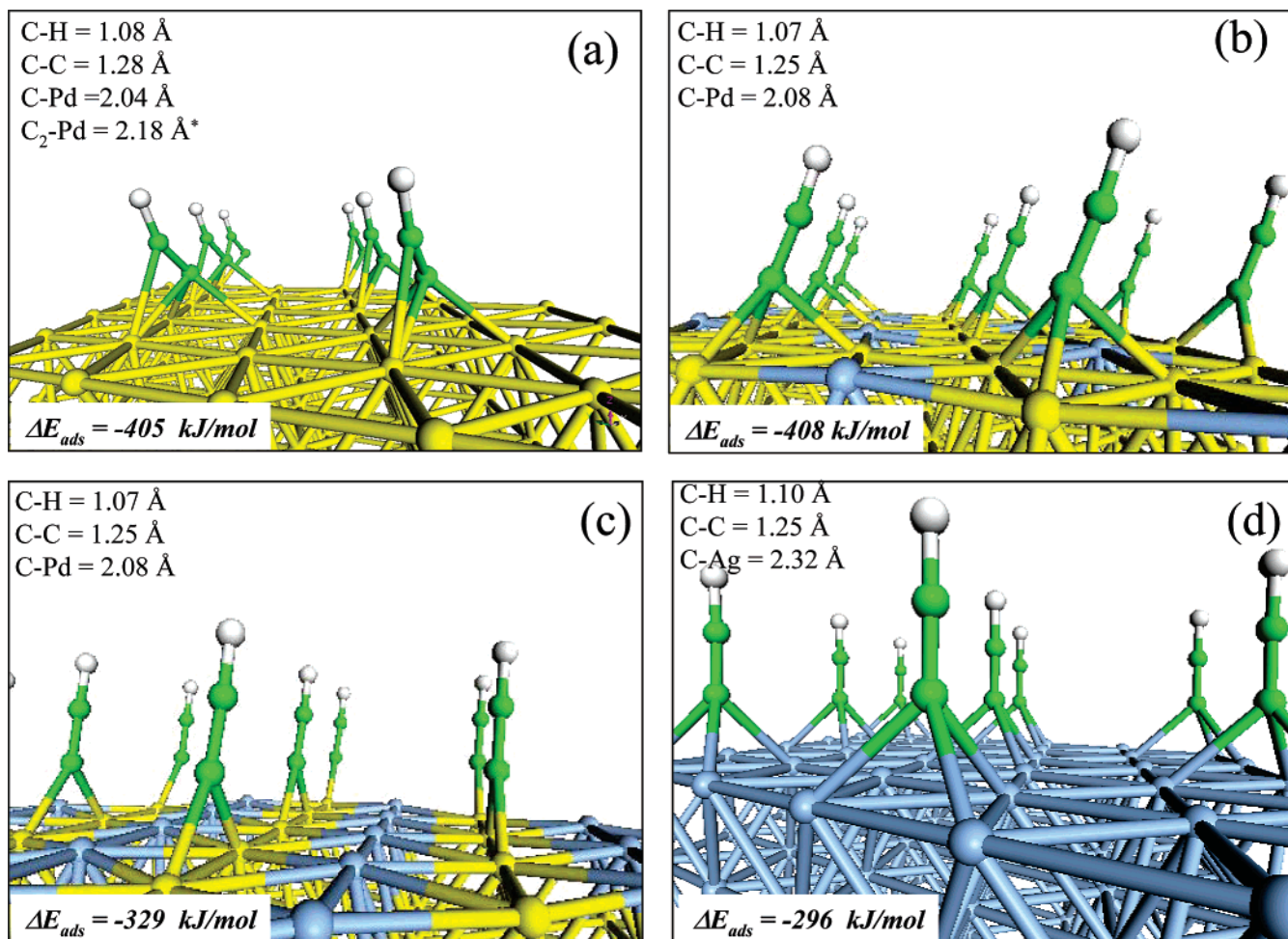


Figure 14. Calculated adsorption geometries of CCH over (a) Pd(111), (b) Pd_{75%}Ag_{25%}/Pd(111), (c) Pd_{50%}Ag_{50%}/Pd(111), and (d) Ag(111).

the kinetics over the 50% surface alloy and will report those results in a future publication.

D. Comparing Acetylene and Ethylene. As was discussed in the introduction, some of the first hypotheses concerning the enhanced hydrogenation selectivity of acetylene to ethylene suggested that alloying Pd with Ag would significantly weaken the adsorption of ethylene and drive it from the surface. The results found herein can be used to begin to test this idea as well as others concerning the selectivity. The adsorption energies for acetylene, presented in Table 1, appear to be much more sensitive to changes in the alloy composition than those for ethylene. This is ascribed to the fact that acetylene prefers to adsorb at the 3-fold (fcc) sites, which are the first sites removed when the alloy composition is increased. In addition, acetylene demonstrates a higher degree of directional bonding. It is therefore much more sensitive to changes in the adsorption site than ethylene is. The change in the binding energy for ethylene to move from the di- σ to a π -bound site is only about 20 kJ/mol,³⁸ whereas the change in the acetylene binding energy in moving from the 3-fold fcc site to a bridge site was found to be nearly 50 kJ/mol.

The calculations carried out here, however, were all performed at somewhat lower coverages (0.25 ML) to assess the intrinsic energetics. The surface coverages under more realistic conditions will be higher where the lateral interactions between adsorbates become appreciable.^{57,58} In previous results, for example, we showed that under more realistic operating conditions the π -bound ethylene mode is more likely the reactive intermediate because it is more weakly held to the surface than the di- σ mode

on Pd(111).³⁸ The binding energy of ethylene on Pd at the π -bound site at higher coverages was found to be about 30 kJ/mol, which was strong enough to allow an appreciable number of ethylene molecules to hydrogenate rather than desorb.^{57,58} To begin to understand the influence of coverage effects, we examined the changes in the binding energies of ethylene and acetylene on the Pd_{50%}Ag_{50%} alloy at the 0.25 ML coverage that had already been reported and at the 0.33 ML coverage. The calculated binding energy for acetylene decreases from -126 to -60 kJ/mol, whereas the binding energies for ethylene decrease from -70 to -17 kJ/mol as the coverage is increased from 0.25 to 0.33 ML. Both acetylene and ethylene demonstrate considerable lateral interactions. These interactions are enhanced on the alloy over those on the pure Pd(111) surface. This weakening in the hydrocarbon adsorption energy should help to increase the intrinsic rates of hydrogenation for both species, assuming that the more weakly bound intermediates more readily react with hydrogen than the more strongly bound intermediates. An important point to note, however, is that the adsorption energy of ethylene on the Pd_{50%}Ag_{50%} alloy at these higher coverages drops to only 17 kJ/mol. This is half of the value of the binding energy of ethylene at the lower (0.25 ML) surface coverage on Pd(111). The binding energy now is weak enough that the rate of desorption of ethylene may begin to overtake the rate of ethylene hydrogenation. The adsorption energy for acetylene on the Pd_{50%}Ag_{50%} alloy, however, is still over 60 kJ/mol. Its rate of desorption should be appreciably slower than that for ethylene, thus allowing the rate of hydrogenation to compete with the rate of desorption.

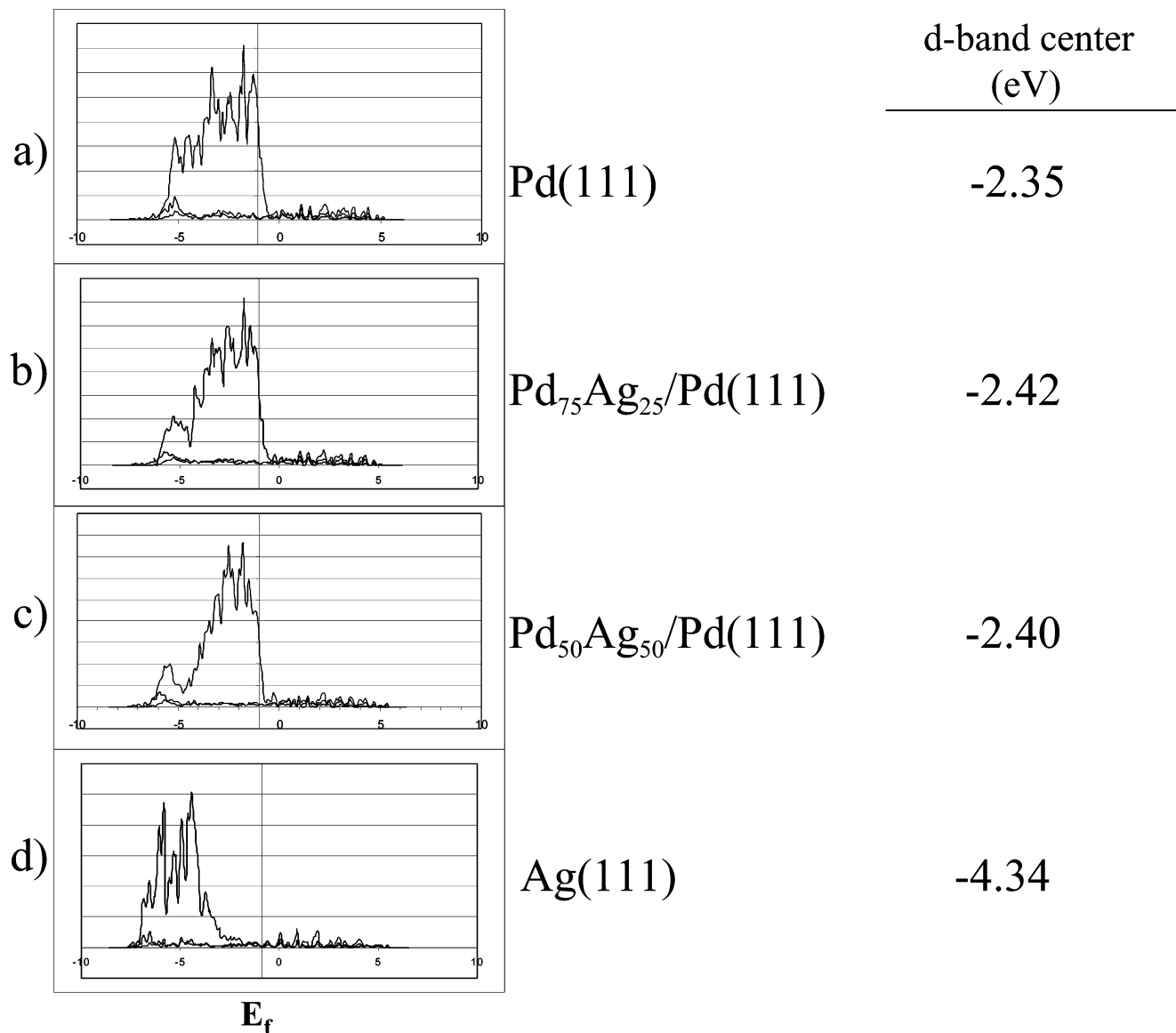


Figure 15. Projected s-, p- and d-band densities of states (DOS) and d-band centers for the Pd surface atom in (a) Pd(111), (b) Pd₇₅Ag₂₅/Pd(111), (c) Pd₅₀Ag₅₀/Pd(111), and (d) the Ag atom in Ag(111).

TABLE 4: Calculated Reaction Energies in kJ/mol of the Surface Elementary Reactions over the Different Surfaces

reaction type	elementary reaction	Pd(111)	Pd ₇₅ Ag ₂₅ /Pd(111)	Pd ₅₀ Ag ₅₀ /Pd(111)	Ag(111)
(a) bond-breaking reactions	H ₂ (g) → 2H*	-82	-76	-77	17
	C ₂ H ₂ * → CCH* + H*	90	82	121	77
	C ₂ H ₃ * CCH ₂ * → + H*	12	28	52	139
	CCH* → C* + CH*	-7	3	85	599
	CH* → C* + H*	50	52	68	170
(b) bond-forming reactions	C ₂ H ₂ * + H* → C ₂ H ₃ *	-3	2	7	-121
	C ₂ H ₂ * + H* → C ₂ H ₄ *	-42	-55	-92	-171
	C ₂ H ₄ * + H* → C ₂ H ₅ *	20	17	20	8
	C ₂ H ₅ * + H* → C ₂ H ₆ *	-12	-20	-33	-116
	CCH ₂ * + H* → CCH ₃ *	-56	-81	-76	-50
	CCH ₃ * + H* → HCCH ₃ *	53	47	43	-44
	CH* + H* → CH ₂ *	17	19	-39	-102
	CH ₂ * + H* → CH ₃ *	-28	-35	-41	-157

The results that we presented earlier in the paper suggested that the rate of acetylene hydrogenation may be more favored over the alloy than ethylene hydrogenation. If we also consider the fact that ethylene may want to desorb preferentially over the higher alloy compositions, this would suggest that there would be a significant increase in the overall selectivity of acetylene to ethylene compared to the hydrogenation of ethylene to ethane.

V. Conclusions

First-principles DFT studies were used to establish and quantify the effects of alloying Pd with Ag on the binding energies of various C₁H_y and C₂H_y intermediates and the overall hydrogenation energies for these intermediates. The addition of Ag to a Pd(111) surface weakens the binding energies for all of the C₁ and C₂ intermediates studied herein. This is due to

both electronic and geometric effects. The binding energy becomes progressively weaker with increases in the Ag composition. An electronic analysis of the alloyed substrates shows that there is in general a decrease in the local density of states of the Pd surface sites upon alloying with Ag and a shift in the d-band center of the Pd atoms away from the Fermi level. In general, this agrees with the Hammer–Nørskov model,¹ which would indicate that there should be a decrease in the adsorbate interaction energies. There are, however, some deviations from this model that may be the result of the interactions between s and p states.

Isolating electronic effects from geometric effects indicates that the presence of Ag at nearest-neighbor sites that are not directly involved in binding the adsorbate acts to weaken the binding energy by only 7 kJ/mol on average. Increasing the number of Ag atoms increases this value slightly. Geometric effects, however, are much more pronounced and range from 65 to 200 kJ/mol depending on the adsorbate, its binding mode, and the number of Ag atoms in the adsorption ensemble. The adsorbate–Ag bonds are considerably weaker than the adsorbate–Pd bonds. In a number of cases, this changes the preferred adsorption site so as to maximize their interactions with the C_xH_y adsorbates and Pd and minimize their direct contact with Ag atoms. Acetylene, for example, shifts from the 3-fold fcc site on the Pd(111) surface to the Pd₂-bridge site on the Pd_{50%}Ag_{50%}(111) surface. Changes in the adsorption energy tend to scale with the relative binding energy of the specific adsorbate.

Changes in the binding/adsorption energies subsequently impact the overall reaction energies for both bond-making and bond-breaking elementary steps. The weaker binding energies enhance bond-forming reactions such as hydrogenation. The more weakly bound C_xH_y and atomic hydrogen intermediates on the alloy surfaces will have a greater propensity to react than the more stable and strongly bound intermediates on the Pd(111) surfaces. In addition, the overall energies for the unselective bond C–H and C–C bond-breaking reactions are more endothermic and will therefore be more likely inhibited by increases in the Ag composition.

The results help to advance ideas on the mechanism by which Ag promotes acetylene hydrogenation. The results suggest that increasing the Ag coverage increases the overall favorability for acetylene hydrogenation. Ethylene, however, is more weakly bound to the surface. A decrease in its adsorption energy may drive it from the surface before it can go on to form ethane. Furthermore, the dissociative adsorption of molecular hydrogen, which is required for additional hydrogenation, becomes less favorable with increasing surface Ag content. There is thus an optimum balance of surface Pd and Ag ratios that is needed for optimum activity and selectivity of the catalyst. These later ideas, however, will clearly depend on the activation barriers and the magnitude of the actual rate constants for these elementary steps.

Acknowledgment. We kindly acknowledge The Dow Chemical Company for the financial support of this work. The Legion Computing group of the Computer Science Department at the University of Virginia and the NCSA supercomputing center at Illinois are also acknowledged for computing resources. We also acknowledge helpful discussions with Drs. Qingfeng Ge, Michael Palmer, and Sanket K. Desai.

References and Notes

- Hammer, B.; Morikawa, Y.; Nørskov, J. K. *J. Phys. Rev. Lett.* **1996**, 76, 2141.
- Coq, B.; Figueras, F. *J. Mol. Catal. A: Chem.* **2001**, 173, 117.
- Sárkány, A.; Horváth, A.; Beck, A. *Appl. Catal., A* **2002**, 229, 117.
- Sárkány, A. *Appl. Catal., A* **1997**, 165, 87.
- Huang, D. C.; Chang, K. H.; Pong, W. F.; Tseng, P. K.; Hung, K. K.; Huang, W. F. *Catal. Lett.* **1998**, 53, 155.
- Brown, M. W.; Penlidis, A.; Sullivan, G. *Can. J. Chem. Eng.* **1991**, 69, 152.
- Thanh, C. N.; Didillon, B.; Sarrazin, P.; Cameron, C. Selective Hydrogenation Catalyst and a Process Using that Catalyst. U.S. Patent, 2000.
- Jin, Y.; Datye, A. K.; Rightor, E.; Gulotty, R.; Waterman, W.; Smith, M.; Holbrook, M.; Maj, J.; Blackson, J. *J. Catal.* **2001**, 203, 292.
- Bos, A. N. R.; Bootsma, E. S.; Foeth, F.; Sleyter, H. W. J.; Westerterp, K. R. *Chem. Eng. Process.* **1993**, 32, 53.
- Bos, A. N. R.; Westerterp, K. R. *Chem. Eng. Process.* **1993**, 32, p 1.
- Cheung, T.-T. P.; Johnson, M. M. Alkyne Hydrogenation Process. Eur. Pat. Appl. 1996.
- Molnár, A.; Sárkány, A.; Varga, M. *J. Mol. Catal. A: Chem.* **2001**, 173, 185.
- Maraschin, N. *J. Mod. Plast.* **1997**, 74, B3(2).
- Walsh, K. A. *Chem. Week* **1997**.
- Frevel, L. K.; Kressley, L. J. Selective Hydrogenation of Acetylene in Ethylene and Catalyst Thereof. U.S. Patent, 1957.
- Johnson, M. M.; Walker, D. W.; Nowack, G. P. Selective Hydrogenation Catalyst. U.S. Patent, 1983.
- Meitzner, G.; Sinfelt, J. H. *Catal. Lett.* **1995**, 30, 1.
- Balerna, A.; Deganello, G.; Liotta, L.; Longo, A.; Mobilio, S.; Venezia, A. M. *J. Non-Cryst. Solids* **2001**, 293–295, 682.
- Bond, G. C.; Wells, P. B. *J. Catal.* **1966**, 6, 397.
- Arnett, R. L.; Crawford, B. L. *J. Chem. Phys.* **1950**, 18, 118.
- McGown, W. T.; Kemball, C.; Whan, D. *J. Catal.* **1978**, 51, 173.
- Borodzinski, A.; Golebiowski, A. *Langmuir* **1997**, 13, 883.
- Borodzinski, A.; Cybulski, A. *Appl. Catal., A* **2000**, 198, 51.
- Zhang, Q.; Li, J.; Liu, X.; Zhu, Q. *Appl. Catal., A* **2000**, 197, 221.
- Aduriz, H. R.; Bodnaruk, P.; Dennehy, M.; Gigola, C. E. *Appl. Catal.* **1990**, 58, 227.
- Choi, S. H.; Lee, J. S. *J. Catal.* **2000**, 193, 176.
- Guczi, L.; Schay, Z.; Stefler, G.; Liotta, L. F.; Deganello, G.; Venezia, A. M. *J. Catal.* **1999**, 182, 456.
- Lindlar, H. *Helv. Chem. Acta* **1952**, 35, 446.
- Sales, E. A.; Benhamida, B.; Caizergues, V.; Lagier, J.-P.; Fiévet, F.; Bozon-Verduraz, F. *Appl. Catal., A* **1998**, 172, 273.
- Coultard, I.; Sham, T. K. *Phys. Rev. Lett.* **1996**, 77, 4824.
- Lu, Z. W.; Wei, S. H.; Zunger, A. *Phys. Rev. B* **1991**, 44, 44.
- Dong, W.; Hafner, J. *Phys. Rev. B* **1997**, 56, 15396.
- Eichler, A.; Kresse, G.; Hafner, J. *Surf. Sci.* **1998**, 397, 116.
- Wilke, S.; Scheffler, M. *Phys. Rev. B* **1996**, 53, 4926.
- Clotet, A.; Pacchioni, G. *Surf. Sci.* **1996**, 346, 91.
- Sheth, P. A.; Neurock, M.; Smith, C. M. *J. Phys. Chem. B* **2003**, 107, 2003.
- Fahmi, A.; van Santen, R. A. *Surf. Sci.* **1997**, 371, 53.
- Neurock, M.; van Santen, R. A. *J. Phys. Chem. B* **2000**, 104, 11127.
- Ge, Q.; Neurock, M. *Chem. Phys. Lett.* **2002**, 358, 377.
- Sandell, A.; Beutler, A.; Jaworowski, A.; Wiklund, M.; Heister, K.; Nyholm, R.; Andersen, J. N. *Surf. Sci.* **1998**, 415, 411.
- Nakatsuji, H.; Hada, M.; Yonezawa, T. *Surf. Sci.* **1987**, 185, 319.
- Pallassana, V.; Neurock, M.; Lusvardi, V. S.; Lerou, J. J.; Kragten, D. D.; van Santen, R. A. *J. Phys. Chem. B* **2002**, 106, 1656.
- Løvvik, O. M.; Olsen, R. A. *J. Chem. Phys.* **2003**, 118, 3268.
- Kresse, G.; Furthmuller, J. *Phys. Rev. B* **1996**, 54, 11 169.
- Kresse, G.; Hafner, J. *J. Phys.: Condens. Matter* **1994**, 6, 8245.
- Perdew, J. P.; Chevary, J. A.; Vosko, S. H.; Jackson, K. A.; Pederson, M. R.; Singh, D. J.; Froehling, C. *Phys. Rev. B* **1992**, 46, 6671.
- Dunphy, J. C.; Rose, M.; Behler, S.; Ogletree, D. F.; Salmeron, M. *Phys. Rev. B* **1998**, 57, R12707.
- Sellars, H. *J. Phys. Chem.* **1990**, 94, 8329.
- Pacchioni, G.; Lambert, R. M. *Surf. Sci.* **1994**, 304, 208.
- Mitsui, T.; Rose, M. K.; Fomin, E.; Ogletree, D. F.; Salmeron, M. *Surf. Sci.* **2003**, 540, 5.
- Pallassana, V.; Neurock, M. *J. Catal.* **2000**, 191, 301.
- Stacchiola, D.; Azad, S.; Burkholder, L.; Tysoe, W. T. *J. Phys. Chem. B* **2001**, 105, 11233.
- Stacchiola, D.; Burkholder, L.; WT, T. *Surf. Sci.* **2002**, 511, 215.
- Tysoe, W. T.; Nyberg, G. L.; Lambert, R. M. *Surf. Sci.* **1983**, 135, 128.
- Tysoe, W. T.; Nyberg, G. L.; Lambert, R. M. *J. Phys. Chem.* **1986**, 90, 3188.
- Kesmodal, L. L.; Waddill, G. D.; Gates, J. A. *Surf. Sci.* **1983**, 138, 464.
- Neurock, M.; Mei, D. *Top. Catal.* **2002**, 20, 5–23.
- Mei, D.; Hansen, E. W.; Neurock, M. *J. Phys. Chem. B* **2003**, 107, 798–810.